Lower Telychian (Silurian) species of *Parapetalolithus* from the *linnaei*, *turriculatus* and *crispus* biozones in the Prague Synform: taxonomy in the light of astogeny and intraspecific variability

Zuzana Strossová

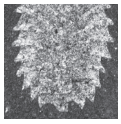

The astogeny and intraspecific variability of the rhabdosomes of six species of the biserial graptolite genus *Parapetalolithus* are described, based upon rich and well-preserved material mostly from the classic Želkovice and Litohlavy localities of the lower Telychian Litohlavy Formation (Prague Synform, Czech Republic). The previous systematic classification of *Parapetalolithus* species has been markedly influenced by the considerable morphological variability of rhabdosomes which is recorded herein within similarly preserved material from the same locality. This formerly resulted in excessive division into separate species and subspecies. Based upon morphometric measurements and subsequent revision, three species and subspecies (*P. clavatus*, *P. elongatus linearis* and *P. conicus*) are synonymized and the following six species are retained: *P. ovatus*, *P. elongatus*, *P. hispanicus*, *P. palmeus*, *P. altissimus*, and *P. tenuis*. This is the first detailed study documenting and comparing the astogeny of several *Parapetalolithus* species, which has a notable impact on their systematic classification and identification and for the first time enables species determination of early growth stages. • Key words: graptolites, stratigraphy, colony development, rhabdosome, Barrandian area, Litohlavy Formation.

Strossová, Z. 2024. Lower Telychian (Silurian) species of *Parapetalolithus* from the *linnaei*, *turriculatus* and *crispus* biozones in the Prague Synform: taxonomy in the light of astogeny and intraspecific variability. *Bulletin of Geosciences 99*(*1*), 43–71 (17 figures, 1 table). Czech Geological Survey, Prague. ISSN 1214-1119. Manuscript received August 30, 2023; accepted in revised form February 26, 2024; published online April 14, 2024; issued April 14, 2024.

Zuzana Strossová, Institute of Geology and Palaeontology, Faculty of Science, Charles University, Albertov 6, Prague, 128 43, Czech Republic & Department of Palaeobiology and Palaeoecology, Institute of Geology, Academy of Sciences of the Czech Republic, Rozvojová 269, 165 00 Praha 6, Czech Republic & Czech Geological Survey, Klárov 3, 118 21 Prague 1, Czech Republic; strossova@natur.cuni.cz

Graptolites are extinct representatives of the class Pterobranchia. They represent one of the most biostratigraphically important groups of the Silurian and are the most important in offshore environments. The occurrences of individual species and assemblages of species enable the establishment of biozones, the duration of which in the best cases are only hundreds of thousands of years (Maletz 2017, Štorch 2023).

Geological and palaeontological investigations have been carried out in the Prague Synform since the 18th century. Barrande (1850) and Suess (1851) were the first to describe graptolites from the Prague Synform. However, Bouček (1933, 1937) was the first to apply modern biostratigraphical methods to graptolites in this region, primarily focusing on the Ordovician and Silurian.

Bouček & Přibyl (1941a, b) distinguished two broad morphological groups within the genus *Petalolithus* Suess, 1851. Their "Group of *Petalolithus palmeus*" (Bouček & Přibyl 1941a) comprised species subsequently referred to the genus *Parapetalolithus* by Koren' & Rickards (1996). Lenz *et al*. (2018) differentiated *Parapetalolithus* from *Petalolithus* (*P. folium* Group of Bouček & Přibyl 1941b) by the absence of an ancora and reduced or absent partial septum on the obverse side of the rhabdosome. Many *Parapetalolithus* species are important biostratigraphical markers. Among the most important are *P. palmeus* Barrande and *P. hispanicus* Haberfelner, which have been used in Bohemia to subdivide the *linnaei* Biozone (the lowermost Telychian biozone in Bohemia) into the eponymous *palmeus* and *hispanicus* subzones.

In general, the classification of graptolites is strongly influenced by the type of preservation, the degree of intraspecific variability, and the principle of convergence. These reasons caused (and still cause) the frequent establishment of new species, which, however, later turn out to be junior synonyms of previously established species. The genus *Parapetalolithus* is no exception, and Bouček & Přibyl (1941a) and Schauer (1971) already pointed out this problem. One of the solutions to this problem is to study the astogeny, *i.e*. the development

of the colony. The term astogeny is equivalent to the ontogeny of a single, non-colonial organism. Most studies that have dealt with the astogeny in graptolites have worked with chemically isolated material (*e.g.* Lenz & Kozłowska-Dawidziuk 2004, Maletz 2017). This present work takes advantage of the abundant occurrence of well-preserved diagenetically flattened specimens of the widely distributed lower Telychian genus *Parapetalolithus* Koren' & Rickards, 1996 in the black shales of the Litohlavy Formation (Prague Synform, Central Bohemia, Czech Republic), to study these issues more comprehensively. The overall characteristics and measurable parameters of the rather flat, foliate rhabdosomes of *Parapetalolithus* have been little influenced by diagenetic flattening and thus their study provides datasets little biased by post-mortem deformation.

The present study outlines: (i) a revision and critical evaluation of all established species of the genus *Parapetalolithus* recorded from the Prague Synform; (ii) a detailed study of the astogeny of all species of *Parapetalolithus*, including their intraspecific variability; (iii) the importance of individual morphometric parameters for differentiation/synonymization of species; (iv) the identification of individual species from juvenile specimens, which has generally not previously been possible. A discussion of the possible evolutionary relationships of selected *Parapetalolithus* species from the *linnaei*, *turriculatus* and *crispus* biozones is included.

Geological setting

The graptolites studied came from both historical and new material collected in the lower Telychian *linnaei*, *turriculatus* and *crispus* biozones (see Fig. 1) exposed at Želkovice near Libomyšl, Litohlavy near Králův Dvůr and Dvorský mlýn near Koněprusy in the southwestern part of the Silurian outcrop area preserved in Central Bohemia southwest of Prague (Fig. 2).

The Ordovician–middle Devonian succession preserved in Central and Western Bohemia, Czech Republic on the Cadomian basement of the Teplá–Barrandian block was described by Havlíček (1981, 1982) as the sedimentary and submarine volcanic infill of a narrow, linear depression developed in the course of syn-sedimentary rifting associated with a stepwise breakdown of the northwestern margin of the Gondwanan mainland. Vacek & Žák (2017) regarded the Prague Basin as

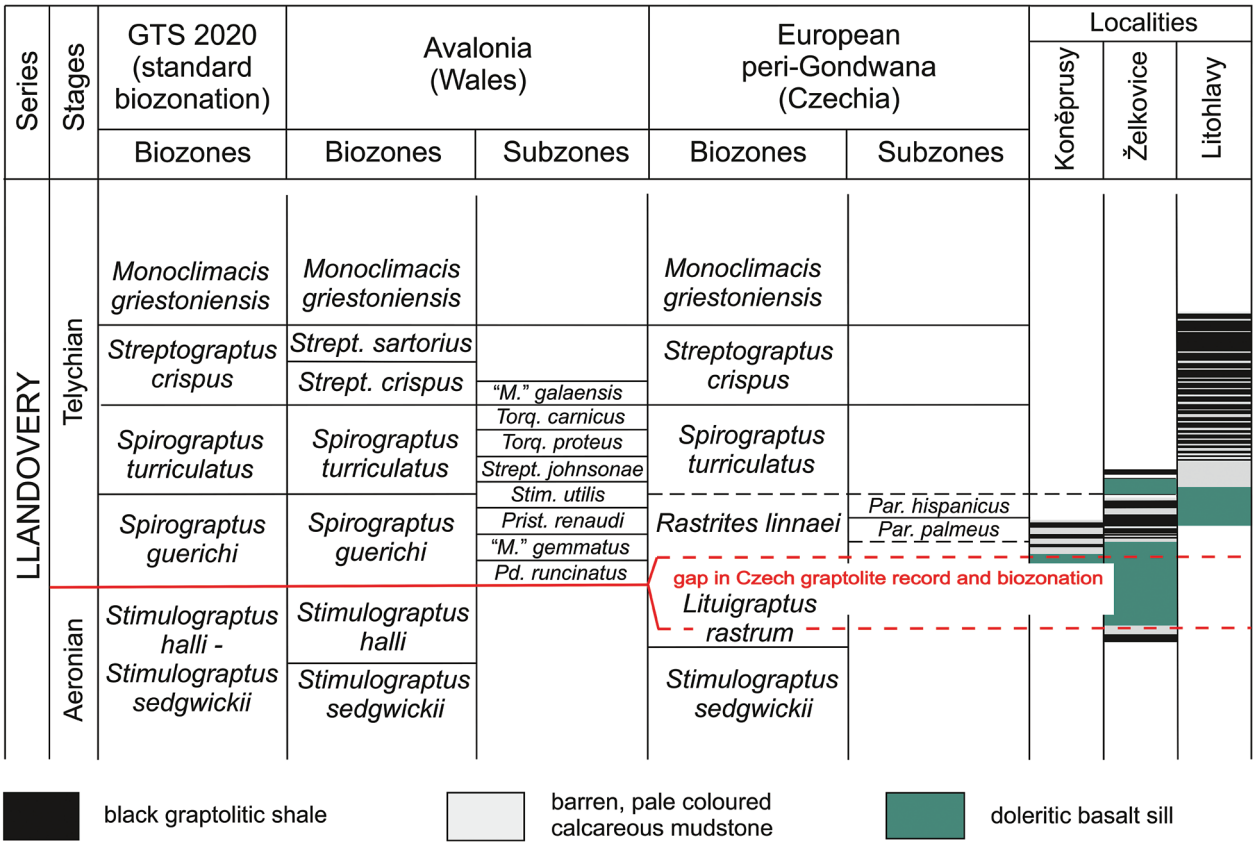

Figure 1. Stratigraphic/sedimentary chart and biozonation of the key sections, showing the distribution of graptolitic and non-graptolitic strata in the Prague Synform. Modified from Štorch *et al.* (in print).

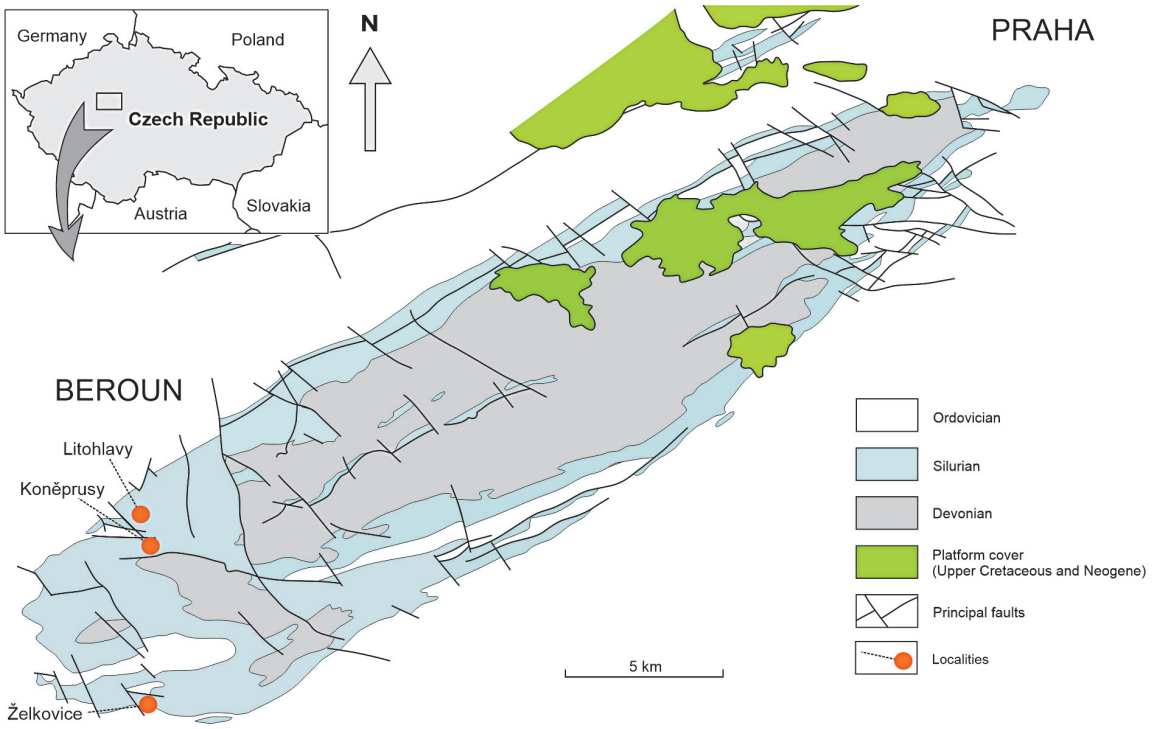

Figure 2. A simplified geological map of the Lower Palaeozoic of the Prague Basin, including localities: Litohlavy near Králův Dvůr, Koněprusy, and Želkovice. These localities yielded the described graptolite material. Base map provided by Š. Manda.

a narrow, fault-bounded graben developed on the deformed and partly eroded Cadomian accretionary wedge. They interpreted the Prague Basin as part of an extensive peri-Gondwanan passive margin, and its origin coheres with the early Palaeozoic extension of the Rheic Ocean. The Prague Basin was formed in the Tremadocian and came to an end in the Givetian (Devonian), when it was uplifted at the dawn of the Variscan Orogeny and its infill became part of the Variscan Orogenic belt (Havlíček 1981, Vacek & Žák 2017). Subsequently, the Variscan mountain belt was eroded and peneplenized gradually. The Prague Synform, as defined by Melichar (2004), is a geological structure represented by an erosional relict of the ancient Prague Basin extending NE–SW between Starý Plzenec and Brandýs nad Labem. In the northeast, its Ordovician succession continues far below the covering Cretaceous platform sedimentary rocks. The central part is formed by sedimentary rocks of Silurian and Devonian age, whereas the peripheral part consists of Ordovician rocks (Melichar 2004, Röhlich 2007). The Silurian succession conformably overlies the Upper Ordovician strata and consists of five formations: the Želkovice, Litohlavy, Motol, Kopanina, and Požáry Formation (see Chlupáč *et al*. 1998 for review).

The Litohlavy Formation, defined by (Kříž 1975), was named after the classical Barrande's locality Litohlavy Mill near Králův Dvůr.

The whole unit is developed as alternating pale-coloured mudstones and black shales. After Štorch (2023), this unit comprises the *R. linnaei*–lowermost *O. spiralis* biozones. However, doleritic basalt sills sandwich the black shale succession of the Litohlavy Formation in many outcrops and sections. Sedimentation took place continuously in the southeastern and northwestern limbs of the Prague Synform. However, the central segment of the Prague Synform, that crops out *e.g*. at Velká Ohrada or Praha-Pankrác, exhibits a considerably long submarine gap in sedimentation (Štorch 2006). The entire Želkovice Formation and the lower part of the Litohlavy Formation are missing. The lower part of the Telychian Stage is completely missing and sedimentation resumed only with a massive layer of pale-coloured heavily mottled calcareous mudstone overlain by a black shale containing a graptolite assemblage marked by the biozonal index species *Monoclimacis griestoniensis* (Kříž 1975, 1992; Štorch 2023).

Material and methods

This study is based on 1,092 specimens of lower Telychian *Parapetalolithus*, of which the 181 best-preserved rhabdosomes were selected for precise measurements of morphological characters (Fig. 3). Specifically,

33 specimens of *P. palmeus* (23 adults, 10 juvenile stages), 33 specimens of *P. elongatus* (27 adults, 6 juveniles), 48 specimens of *P. ovatus* (26 adults, 22 juveniles), 29 specimens of *P. hispanicus* (21 adults, 8 juveniles), 7 specimens of *P. altissimus* (5 adults, 2 juveniles) and 33 specimens of *P. tenuis* (27 adults, 6 juveniles) were measured. The studied material was acquired by the present author during in situ sampling of the lower Litohlavy Formation at the Želkovice and Litohlavy sections. Further specimens came from unpublished material collected at Želkovice, Litohlavy and Koněprusy by P. Štorch as well as from the collections of J. Barrande and B. Bouček housed in the National Museum, Prague and the Czech Geological Survey, Prague. The type material of *P. conicus*, *P. ovatus*, *P. tenuis*, *P. palmeus palmeus*, *P. palmeus clavatus*, *P. elongatus elongatus* and *P. elongatus linearis* (see Fig. 4), described by Barrande (1850), Perner (1897) and Bouček & Přibyl (1941a), was examined in this study.

The graptolites are preserved on black shale surfaces in the majority of cases as flattened silvery impressions, rarely partially pyritized and preserved in low relief.

The Želkovice locality occurs along a field tract east of a large old farm in Želkovice, near Libomyšl. Minor outcrops were extended by excavation providing access to the black shales and pale-coloured mudstones of the lowermost part of the Litohlavy Formation, assigned to the *Rastrites linnaei* Biozone. This site provided the type material of many taxa described by Barrande (1850), Perner (1897), Bouček (1932), Bouček & Přibyl (1941a, b), and Bouček & Münch (1944) including that of the *Parapetalolithus* species revised by this study: "*Graptolithus*" *ovatus*, "*Graptolithus*" *palmeus*, "*Petalograptus*" *conicus*, "*Petalolithus*" *palmeus clavatus*, "*Petalolithus*" *elongatus elongatus* and "*Petalolithus*" *elongatus linearis.*

A small, nowadays overgrown outcrop exposed on the west side of a local road from Koněprusy to Suchomasty Creek valley, near Havlíčkův (formerly Dvorský) Mill yielded some graptolites indicating the *P. palmeus* Subzone of the *linnaei* Biozone, including the index species *P. palmeus*.

The lower part of the Litohlavy Formation exposed by a local railroad opposite the Litohlavy water reservoir Suchomasty, 1.5 km west of Králův Dvůr, is located only

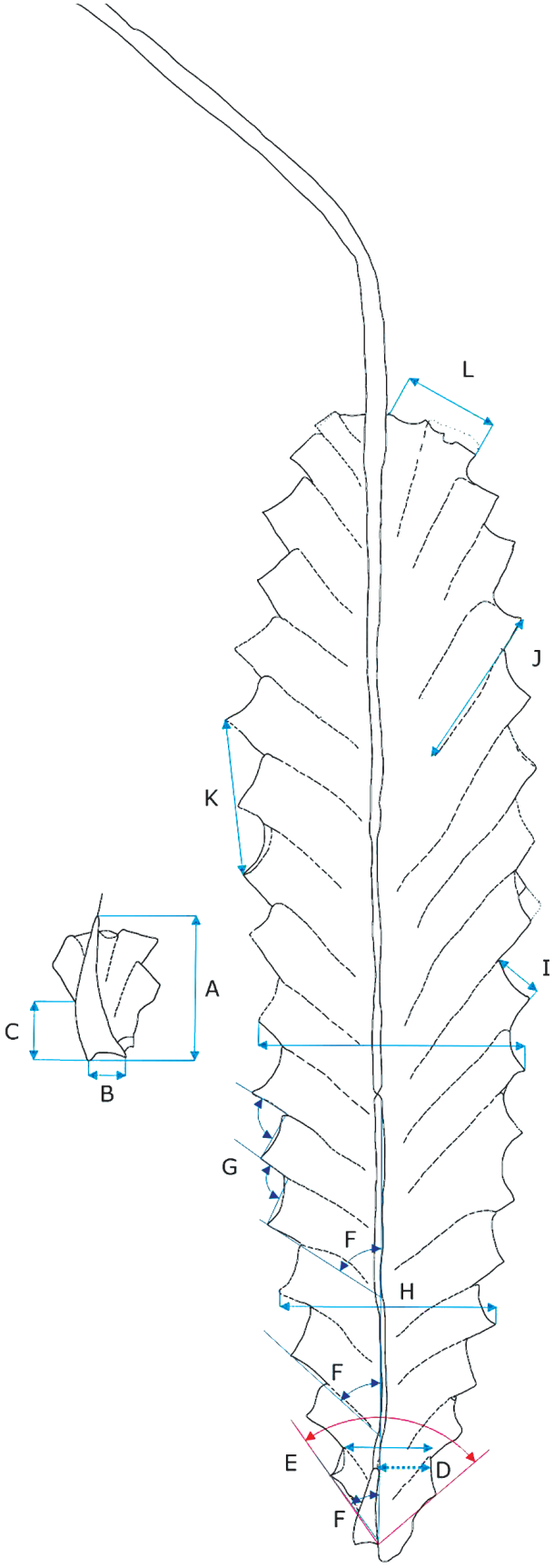

Figure 3. An overview of the measured parameters used in this study. A – sicula length; B – apertural width of the sicula; C – length of the free dorsal wall of the sicula; D – the order of the thecae which the apex of sicula reaches; E – apical angle measured at the 1st pair of thecae; F – angle of divergence (abbreviated AD) at the 1st–6th pair of thecae; G – angle of apertures (abbreviated AP) between 5th–7th thecae; H – dorso-ventral width (abbreviated DVW) at the 1st–7th pair of thecae; I – width of apertures at the 1st–7th pair of thecae; J – thecal length; K – $2TRD_2$, $2TRD_5$, $2TRD_{10}$; L – number of incomplete thecae at the distal end of the rhabdosome.

tens of metres from the nowadays inaccessible graptolite locality where J. Barrande acquired many of the graptolites described in his monograph (Barrande 1850) including the type material of "*Graptolithus*" *tenuis*. The exposed section comprises the upper part of the *Spirograptus turriculatus* Biozone and the *Streptograptus crispus* Biozone.

The material was studied and photographed when dry, or submerged in ethanol, using an Olympus SZX 16 stereo-microscope and an Olympus SZX 10 stereo-microscope fitted with a Canon EOS 2000D camera at the Institute of Geology of the Academy of Sciences. Measurements were carried out using the QuickPHOTO MICRO software; line drawings were made using the Adobe Photoshop software.

The analysis used in this study is based on the following 12 morphological characteristics (Fig. 3): (A) sicula length; (B) apertural width of the sicula; (C) length of the free dorsal wall of the sicula; (D) theca(e) which the apex of sicula reaches; (E) apical angle measured at the 1st thecal pair; (F) angle of divergence (abbreviated AD) at the 1st–6th thecal pairs; (G) angle of apertures (abbreviated AP) between 5th–7th thecae; (H) rhabdosome dorso-ventral width (abbreviated DVW) at 1st–7th thecae; (I) width of apertures at 1st–7th thecae; (J) thecal length; (K) two thecae repeat distance (2TRD *sensu* Howe 1983) at th2, 5 and 10; (L) number of incomplete thecae at the distal end of the rhabdosome. The first set of measurements included up to 32 characteristics and morphological features for each specimen (excluding juvenile stages), which were utilized in subsequent analyses.

For selected parameters, which later turned out to be of key significance, the mean values (marked by M) were calculated from all measured specimens (n) of each species listed in Table 1.

The measured and figured specimens are housed in the collections of the National Museum, Prague (type material of J. Barrande, J. Perner, B. Bouček, and A. Přibyl prefixed L), and Czech Geological Survey (collections prefixed PŠ and ZAZ).

Systematic palaeontology

The results of measurements of rhabdosome dorso-ventral width (DVW) and angle of divergence (AD) at the 3rd and 5th thecal pairs for all described species are shown in Table 1 and in Figs 14–17.

Superfamily Retiolitoidea Lapworth, 1873
Family Retiolitidae Lapworth, 1873
Subfamily Petalolithinae Bulman, 1955

Genus *Parapetalolithus* Koren' & Rickards, 1996

Type species. – *Parapetalolithus dignus* Koren' & Rickards, 1996. Holotype: CNIGR 124/12879 Zhaksy-Kargala Valley, southern Urals, Russia, from the *guerichi* Biozone.

Diagnosis. – Non-ancorate biserial rhabdosome with pattern I proximal development, first thecal pair V-shaped, thecae moderately to steeply inclined, straight to slightly ventrally curved, with more or less everted, nearly ventrally facing apertures. Nema free and central or embedded in obverse wall, commonly extended into a prominent nematularium (emended from Lenz *et al*. 2018).

***Parapetalolithus palmeus* (Barrande, 1850)**
Figures 4A, H; 5A–O; 6F–H; 13J1–2, M, O

partim 1850 *Grapt. Palmeus* Var. *Lata*; Barrande, pp. 59–63, pl. 3, figs 3–4 (*non* 5–7).
partim 1850 *Grapt. Palmeus* Var. *Tenuis*; Barrande, pp. 59–63, pl. 3, fig. 1 (*non* 2).
partim 1851 *Petalolithus palmeus*. – Suess, pp. 104–105, pl. 8, fig. 1c (*non* a, b).
partim 1897 *Petalograptus palmeus* Barrande. – Elles, pp. 193–195, pl. 14, fig. 4 (*non* 1–3).
non 1897 *Petalograptus palmeus* var. *latus* (Barr.). – Elles, pp. 195–196, pl. 14, figs 5–8.

Table 1. Summary of AD and DVW measurements (in mm). Abbreviations: M – mean value; n – number of specimens.

Species	AD th3			DVW th3			AD th5			DVW th5		
	range	M	n	range	M	n	range	M	n	range	M	n
P. palmeus	48–65	54	23	2.17–2.86	2.44	23	41–61	50	23	2.14–3.51	2.83	23
P. hispanicus	40.4–51.6	44	19	1.32–1.89	1.58	19	33–48.6	41	19	1.71–2.36	1.58	22
P. ovatus	85–110	99	26	2.55–3.79	3.07	26	80–110	89	25	2.72–4.95	3.82	24
P. elongatus	21–29	25	27	1.15–1.46	1.30	27	20–32.6	25	27	1.35–1.74	1.55	27
P. tenuis	26–48	37	27	1.38–2.00	1.67	27	24–45	35	27	1.63–2.31	1.92	27
P. altissimus	37.5–45	42	5	1.57–2.42	1.95	5	33–55	41	5	1.90–2.95	2.48	5

partim 1897 *Diplograptus palmeus* Barrande. – Perner, pp. 3–4, pl. 9, figs 1, 4 (*non* 2).
partim 1908 *Petalograptus palmeus* s.s. (Barrande). – Elles & Wood, pp. 274–275, text-fig. 188a (*non* b, pl. 32, figs 1a–d).
non 1908 *Petalograptus palmeus var. latus* Barrande. – Elles & Wood, pp. 275–276, pl. 32, fig. 2a–f, text-fig. 189a–c.
partim 1908 *Petalograptus altissimus*, sp. nov.; Elles & Wood, pp. 281–282, pl. 32, fig. 7b, ?d (*non* a, c, e), text-fig. 194b (*non* a, c).
1941a *Petalolithus palmeus palmeus* (Barrande 1850). – Bouček & Přibyl, pp. 3–4, pl. 1, figs 1–3, text-fig. 1, figs 1–3.
1941a *Petalolithus palmeus clavatus* n. var.; Bouček & Přibyl, 1941a. pp. 6–8, text-fig. 1, figs 4–5; pl. 1, figs 4–5, pl. 2, fig. 2.
1992 *Petalolithus palmeus* (Barrande, 1850). – Loydell, pp. 47–50, pl. 1, figs 14, 17; text-fig. 13, figs 16, 21 (see for further synonymy).
1998 *Parapetalolithus palmeus* (Barrande). – Gutiérrez-Marco & Štorch, figs 4, 8g.
2000 *Parapetalolithus palmeus* (Barrande). – Štorch *in* Zalasiewicz *et al*., fig. 1.71.
2003 *Parapetalolithus* cf. *palmeus* (Barrande). – Štorch & Massa, figs 5, 17.
2015 *Parapetalolithus clavatus* (Barrande). – Loydell *et al*., fig. 18ag.
2015 *Parapetalolithus palmeus* (Barrande). – Loydell *et al*., figs 16j, 18af.
2021 *Parapetalolithus palmeus* (Barrande, 1850). – Hopfensperger *et al*., figs 1c, f, 3e, g–i, k.
2021 *Petalolithus palmeus* (Barrande, 1850). – Maletz *et al*., fig. 13d.
2021 *Parapetalolithus clavatus* (Bouček & Přibyl). – Maletz *et al*., fig. 13e.

Lectotype. – Figured herein (Fig. 4H), designated by Bouček & Přibyl (1941a, p. 4), Figured by Barrande (1850, pl. 3, fig. 3) and Bouček & Přibyl (1941a, pl. 1, Fig. 2). Specimen NML 27577, from Želkovice, Bohemia.

Material. – Three hundred and ninety-four specimens, from the middle *linnaei* Biozone from Želkovice near Libomyšl and Dvorský Mlýn near Koněprusy.

Diagnosis. – Oblong rhabdosome with a rapidly widening proximal part, reaching the maximum width of 3.3 mm at the 5th–7th thecal pair. Then the width is either maintained or the rhabdosome gets markedly narrower distally. Sicular apex attains the level of the 3rd thecal pair. Thecae are simple tubes with straight interthecal septa and somewhat everted, nearly ventrally facing, straight or gently concave apertures. The thecal overlap is about three-quarters of their length; the overlap is particularly noticeable in older growth stages. The angle of divergence on the 3rd pair of thecae ranges between 48–65°and reaches up to 72° at the 6th thecal pair and then remains constant or slightly decreases in the distal part of mature specimens.

Description. – Rhabdosome is oblong, 15–20 mm long, exceptionally even 25 mm. Sicula length reaches 1.19–1.63 mm. Width of the sicular aperture fluctuates between 0.23–0.4 mm. Length of the free part of the dorsal wall of the sicula ranges from 0.34 to 0.59 mm. Sicular apex attains the 2nd/3rd thecal pair (exceptionally to the 3rd/4th thecal pair) (see Figs 5B, E; 13J). Curvature of the ventral thecal walls of the 1st thecal pair is very moderate. Apical angle measured at the 1st pair of thecae ranges from 61° to 96°, usually between 74–85°. Angle of divergence (AD – Fig. 3) on the 1st thecal pair ranges between 39–55°, on the 3rd thecal pair between 48 and 65° and then the range decreases slightly to 41–61° at the 5th thecal pair. Angle of divergence values of 32–73° were recorded on the 6th pair of thecae. Angle of apertures (AP – Fig. 3) reaches 75–130° between the 5th and 6th thecal pairs and 73–120° between the 6th and 7th thecal pairs. Dorso-ventral width (DVW) increases gradually, but not continuously and uniformly. Initially, DVW increases progressively: the measured values at th1 are 1.38–1.79 mm, for th3 are 1.84–2.86 mm, for th5 2.14–3.51 mm, at th6 2.11–3.61 mm and at the 8th thecal pair 1.94–3.56 mm. Then the DVW begins to decrease gradually, *e.g*. (for specimens with 10 or more thecae): on the 10th thecal pair values reach 1.84–3.49 mm. The width of thecal apertures stays relatively constant and increases only very moderately. The values are 0.25–0.62 mm at the 1st thecal pair, 0.35–0.75 mm at the 3rd thecal pair, 0.47–0.74 mm at the 5th thecal pair and 0.51–0.86 at the 7th thecal pair. More distal thecal apertures show similar values. Thecae overlap by three-quarters of their length in the proximal

Figure 4. Type specimens of *Parapetalolithus* revised in this study. • A – *Petalolithus palmeus clavatus* (Bouček & Přibyl, 1941a), NML 27575. • B – *Petalolithus altissimus* (Elles & Wood, 1908), GSE 5622 (housed at the British Geological Survey), photo kindly provided by D. Loydell. • C – *Petalolithus tenuis* (Barrande, 1950), NML 27569. • D – *Petalolithus elongatus linearis* (Bouček & Přibyl, 1941a), NML 30986. • E – *Petalolithus elongatus elongatus* (Bouček & Přibyl, 1941a), NML 30983. • F – *Petalolithus ovatus* (Barrande, 1950), NML 27579. • G – *Petalolithus conicus* (Bouček, 1932), NML 31400. • H – *Petalolithus palmeus palmeus* (Barrande, 1950), NML 27577. • All specimens originate from the *linnaei* Biozone of Želkovice, except for specimens B (*halli* Biozone, from Black Linn, Glenkiln Burn, Scotland, Great Britain) and C (from the *turriculatus* Biozone from Litohlavy near Králův Dvůr). Scale bars represent 1 mm.

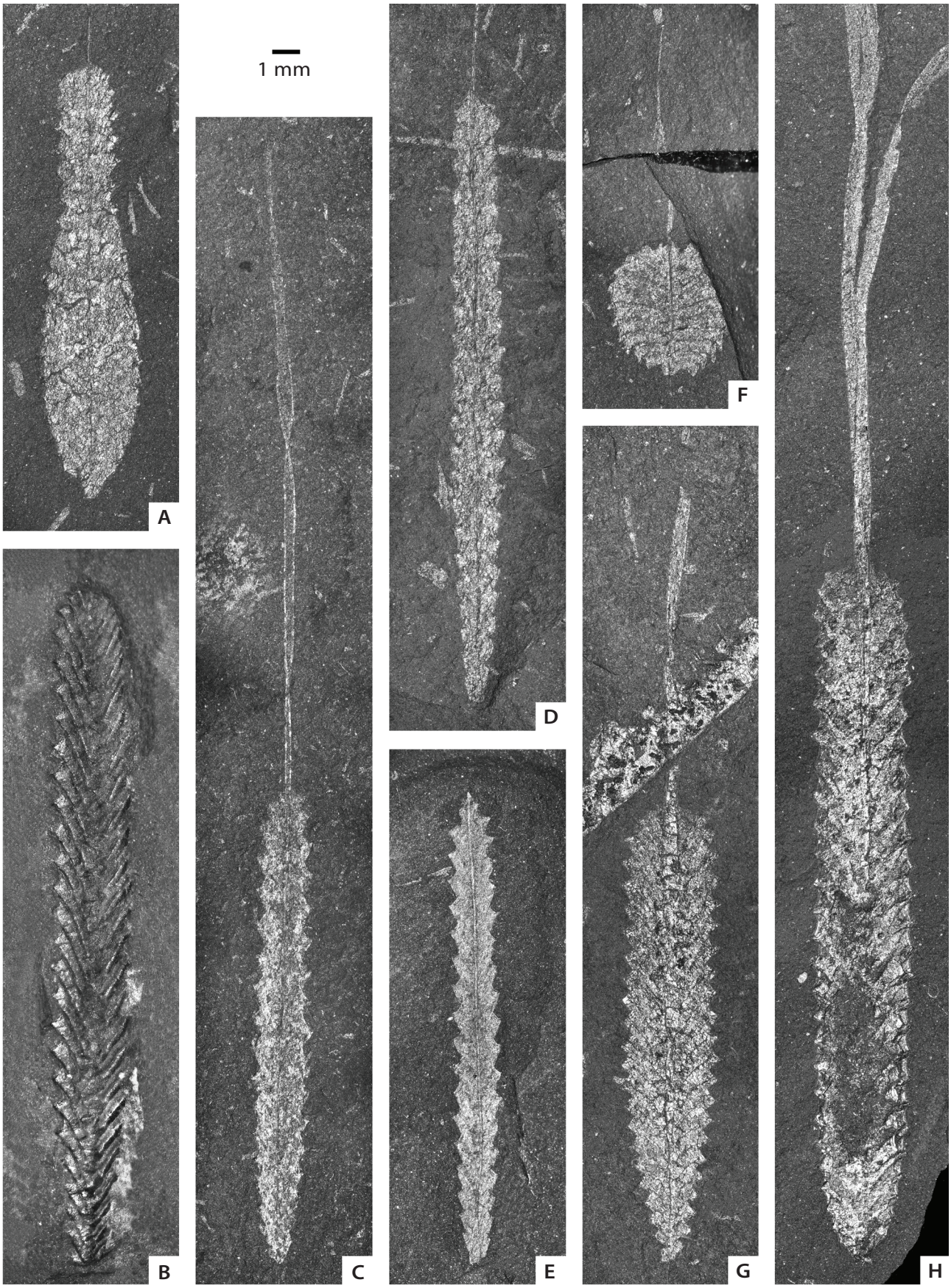
1 mm
A
B
C
D
E
F
G
H

part of the rhabdosome and by more than two-thirds in the distal part of the rhabdosome. The $2TRD_2$ values are 1.15–1.71 mm, $2TRD_5$ values are 1.21–1.69 mm and $2TRD_{10}$ values are 1.13–1.96 mm. At the distal end of the rhabdosome, one pair of incomplete thecae was commonly observed and occasionally two pairs of incomplete thecae. A nematularium was observed in some specimens, generally ribbon-like (twisted or straight) in form, but also as a wider, more complex structure resembling a distalward spreading veil (Fig. 6F, G, H).

The early juveniles of *P. palmeus* are characteristic and distinguishable (from the other species of *Parapetalolithus* studied here and their juveniles) by the significant width of the rhabdosome at the 1st–5th pairs of thecae and AD, which does not differ between juvenile and adult stages (see Fig. 5). The combination of these two parameters gives the characteristic shape of the proximal part of the rhabdosome (more precisely, the first 3 thecal pairs) similar to an inverted, equilateral triangle.

Discussion. – Bouček & Přibyl (1941a) distinguished two varieties/subspecies of *P. palmeus* (Barrande, 1850). "*Petalolithus*" *palmeus clavatus* (Bouček &Přibyl 1941a) was differentiated from the type "variety" based on significant widening of the proximal part of the rhabdosome with respect to the distal part. Except for the relatively greater width and proximal thecal length, however, the other morphological characters are identical between the two subspecies. Bouček & Přibyl (1941a) cited Barrande's (1850) opinion, who had supposed that the ovoid shape of the proximal part recorded in specimens referred by Bouček & Přibyl (1941a) to *P. palmeus clavatus* resulted from deformation. The present study, however, revealed no specific deformation. The relatively wider proximal part of the rhabdosome is not confined to *P. palmeus clavatus*, but may be observed in some mature rhabdosomes of other petalolithine species (e.g. *Parapetalolithus tenuis*, Fig. 12I, L) and *Petalolithus ovatoelongatus* (Bjerreskov 1975, Suyarkova 2017, Štorch *et al*. 2018). The degree of relative widening of the proximal part varies among specimens and thus is not a diagnostic characteristic of a species or subspecies. Both subspecies of *P. palmeus* occur within the same stratigraphical level, with "*clavatus*" morphs being relatively rare.

Parapetalolithus palmeus is known from the *linnaei* or *guerichi* Biozone from many parts of the Silurian world. Loydell (1992) documented the species from Wales (where it ranges into the lowermost *turriculatus* Biozone), Gutiérrez-Marco & Štorch (1998) described it and recognised the *palmeus* Subzone in Spain (Western Iberian Cordillera). Melchin (1998) recorded *P. palmeus* in Arctic Canada, Štorch & Massa (2003) from Libya, and Suyarkova (2017) from the Kaliningrad District.

Loydell *et al.* (2015) described many *Parapetalolithus* species from the El Pintado reservoir sections, Seville Province, Spain. Those with similarities to *P. palmeus* are discussed below.

Parapetalolithus kunkojensis (Paškevičius, 1979) was originally described as a subspecies of *P. palmeus* distinguished by the distal narrowing of the rhabdosome with shorter and less overlapping thecae. The illustration (Paškevičius 1979, pl. 4, fig. 9) shows a different morphology of the rhabdosome in the proximal and distal parts. By contrast, Loydell *et al.* (2015) compared *P. kunkojensis* with *P. hispanicus.* The proximal end of *P. kunkojensis* differs from that of *P. palmeus* in being more acuminate.

Parapetalolithus curvithecatus (Ge, 1990), from the Shuanghechang Formation, lower Telychian of Chengkou, Sichuan, China is also recorded by Loydell *et al*. (2015) from the *guerichi* Biozone of El Pintado reservoir in Spain. However, based on the description and illustrations (p. 769, figs 17k, 18a, b) the Spanish specimens assigned to *P. curvithecatus* strongly resemble juvenile *P. palmeus* in a similar manner to the juvenile specimens assigned by Bouček & Přibyl (1941a) to *P. palmeus clavatus*.

Parapetalolithus mui Loydell *et al*. 2015 (see p. 772, figs 16f, i, p, 18z, ai, ak), is similar to *P. palmeus*, but shows a different morphology of the proximal part of the rhabdosome (*P. mui* has a narrower proximal part than *P. palmeus*). The angle of divergence is, however, similar to *P. palmeus* and some of Figured specimens (especially fig. 16 in Loydell *et al*. 2015) strongly resemble the juvenile stage of *P. palmeus,* but slightly deformed. *Parapetalolithus mui* was also recorded from the *guerichi* Biozone of the Tielugou section in China (Maletz *et al.* 2021, fig. 13a, h) and, according to Loydell *et al*. (2015), from Nanjiang, Sichuan, China and from the northern Canadian Cordillera.

Parapetalolithus sierranortensis (Loydell *et al*. 2015) exhibits a proximal part similar to that of *P. palmeus* (see Loydell *et al*. 2015, fig. 18aq), but Loydell *et al*. (2015) noted that *P. sierranortensis* is narrower than *P. palmeus* (*e.g*. rhabdosome width at $th1^1$ was 0.9 mm).

Figure 5. The astogeny of *Parapetalolithus palmeus* (Barrande, 1950) from the early juvenile stage (Figs A–G) to the adult stage. A – ZAZ 1; B – ZAZ 2; C – ZAZ 3; D – ZAZ 4; E – ZAZ 5; F – ZAZ 6; G – ZAZ 7; H – ZAZ 8; I – ZAZ 9; J – PŠ 469/1; K – ZAZ 10; L – ZAZ 11; M – ZAZ 12; N – ZAZ 13; O – ZAZ 14. All specimens originate from the *linnaei* Biozone, lowermost Litohlavy Formation, Želkovice (1–14) and Koněprusy (15). Scale bars represent 1 mm.

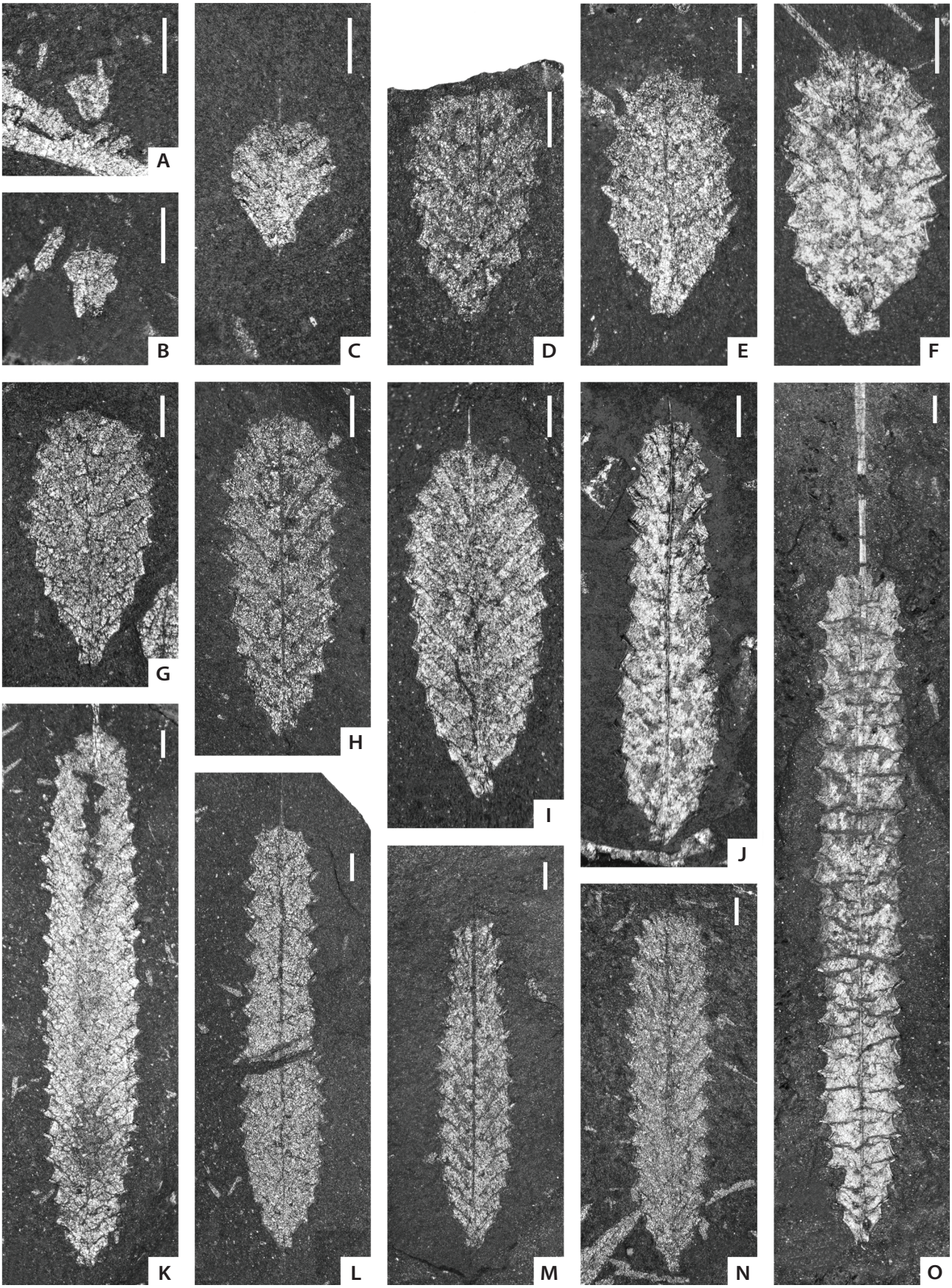
A
B
C
D
E
F
G
H
I
J
K
L
M
N
O

***Parapetalolithus elongatus* (Bouček & Přibyl, 1941)**
Figures 4D, E; 7A–O; 13K, Q1–2

partim 1924 *Diplograptus palmeus* Barrande. – Hundt, p. 58, pl. 2, fig. 24 (*non* figs 25–26).
1941a *Petalolithus elongatus elongatus* n. sp.; Bouček & Přibyl, pp. 10–11, pl. 2, figs 1–2, text-fig. 2, figs 1–5.
1941a *Petalolithus elongatus linearis* n. sp.; Bouček & Přibyl, pp. 11–13, text-fig. 2, figs 6–7.
1992 *Petalolithus elongatus* (Bouček & Přibyl, 1941). – Loydell, pp. 41–42, text-fig. 12, fig. 9 (see for further synonymy).
1998 *Parapetalolithus elongatus* (Bouček & Přibyl). – Gutiérrez-Marco & Štorch, fig. 8q.
2015 *Parapetalolithus elongatus.* – Loydell *et al*., figs 16ad, 18ap.
2015 *Parapetalolithus linearis* (Bouček & Přibyl). – Loydell *et al*., figs 16s, 18ao.
2021 *Parapetalolithus elongatus* (Bouček & Přibyl, 1941). – Hopfensperger *et al*., fig. 3j, m.
2021 *Parapetalolithus elongatus* (Bouček & Přibyl, 1941). – Maletz *et al*., fig. 13m.

Holotype. – Figured herein (Fig. 4E), designated by Bouček & Přibyl (1941a, p. 7, text-Fig. 2, Fig. 1). Specimen NML 30986 from Želkovice, Bohemia.

Material. – One hundred and eighty-nine specimens from the middle *linnaei* Biozone from Želkovice near Libomyšl.

Diagnosis. – Narrow rhabdosome, with relatively constant rhabdosome width from 8th thecal pair. Sicula is long (max. length is 1.9 mm) and its apex reaches the level of the 2nd–3rd thecal pair. Thecae are cylindrical. Thecal apertures are straight, in some cases slightly everted. Angle of divergence on the 3rd pair of thecae ranges between 21–29°.

Description. – Rhabdosome is narrow, 21–27 mm long, exceptionally even 44 mm long. Sicula length reaches 1.22–1.92 mm. Width of the sicula aperture fluctuates between 0.21 and 0.39 mm. Length of the free part of the dorsal wall of the sicula ranges from 0.37 to 0.59 mm. Apex of sicula attains the level of the 2nd thecal pair in adult specimens, but it reaches the 2nd/3rd thecal pair in juveniles. Curvature of the ventral thecal walls of the 1st thecal pair is imperceptible. Apical angle measured at the 1st thecal pair ranges from 47° to 67°, although it usually varies between 50–55°. Angle of divergence (AD – Fig. 3) remains relatively constant, irrespective of colony age. On the 1st thecal pair, the angle is 22–42°, on the 3rd thecal pair between 21–29° and on the 5th and 6th thecal pairs its maximum is 20–32.5° and 20.6°–31.5° respectively. Angle of apertures (AP – Fig. 3) reaches 96°–119° between the 5th and 6th thecal pairs and 100°–123° between the 6th and 7th thecal pairs. Dorso-ventral width (DVW) increases very slightly and from the 8th thecal pair stays practically unchanged. The values for th1 are 0.80–1.05 mm, for th3 1.15–1.46 mm, for th5 1.35–1.74 mm and 1.33–1.85 mm for th6. For the most mature specimens (with 10 or more thecae), th8 and th10 values reached 1.18–1.98 mm and 1.34–2.07 mm, respectively. The width of apertures shows relatively constant values and increases only very slightly. The average values are 0.14–0.33 mm at the 1st thecal pair, 0.14–0.31 mm at the 2nd thecal pair, 0.2–0.35 mm at the 3rd thecal pair, 0.27–0.42 mm at the 5th thecal pair and 0.29–0.38 at the 7th thecal pair. Thecae overlap by approximately one half of their length in both juvenile and adult stages. The $2TRD_2$ values are 1.1–1.72 mm, while $2TRD_5$ and $2TRD_{10}$ values are 1.52–2.22 mm and 1.43–2.09 mm, respectively. At the distal end of the rhabdosome, one pair of incomplete thecae was commonly observed; the growth of two unfinished pairs of thecae occurs only exceptionally (in juvenile stage – see Fig. 7A, E). A nematularium was observed as either a subtle ribbon-like (Fig. 6I) or a very slightly spreading spirally twisted structure (Fig. 6J). The early juveniles of *P. elongatus* are very well-recognisable due to relatively low values of DVW up to the 5th thecal pair, constant AD values in both juveniles and adults and, compared to other studied *Parapetalolithus* species, significantly longer sicula. The overall shape of the proximal part of the rhabdosome, ignoring thecal apertural indentations, to the 3rd–5th pair of thecae may seem to resemble a rectangle (see Fig. 7D, E, F).

Discussion. – Bouček & Přibyl (1941a) recognised two subspecies of their new species *P. elongatus*: *P. elongatus elongatus* and *P. elongatus linearis*. *Parapetalolithus e. linearis* (holotype figured in Fig. 4D) was stated to be

Figure 6. Overview of long, more or less spirally twisted ribbon-like nematularium, either parallel-sided or distalwards slightly widening, which has been recorded in all species studied herein. • A, D – *Parapetalolithus hispanicus* (Haberfelner, 1931); ZAZ 71, ZAZ 74. • B – *Parapetalolithus ovatus* (Barrande, 1850); NML 27579. • C, E – *Parapetalolithus tenuis* (Barrande, 1850); ZAZ 69, ZAZ 67. • F, G, H – *Parapetalolithus palmeus* (Barrande, 1850) possesses wider, presumably more complex nematularium resembling distalward spreading veil; ZAZ 70, NML 27577, ZAZ 14. • I, J – *Parapetalolithus elongatus* (Bouček & Přibyl, 1941a); ZAZ 33, ZAZ 75. • K – *Parapetalolithus altissimus* (Elles & Wood, 1908); PŠ 494. • All specimens originate from the *linnaei* Biozone of Želkovice, except for specimens C, E, K (originate from the *turriculatus* and *crispus* biozones from Litohlavy near Králův Dvůr). Scale bars represent 1 mm.

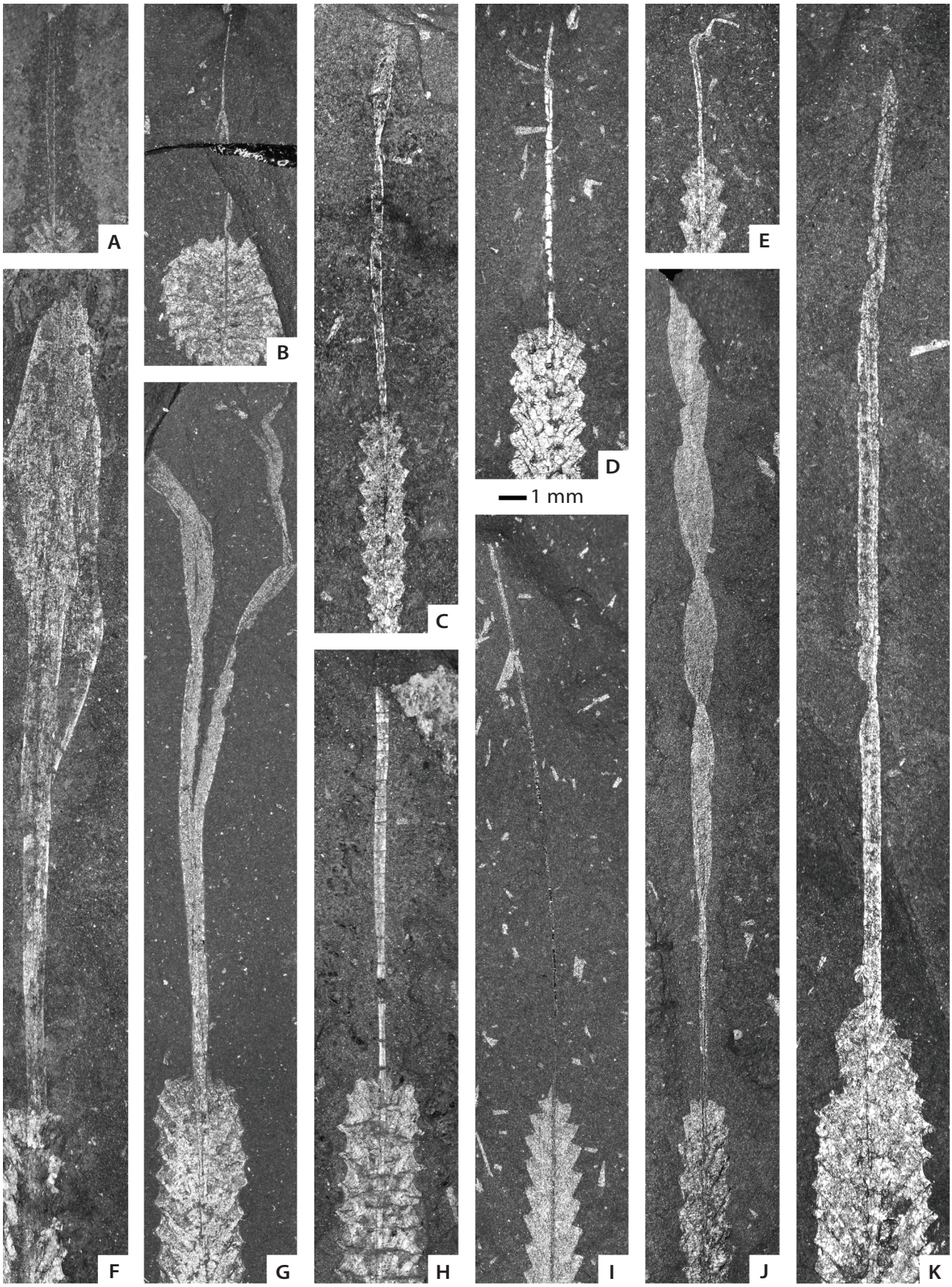
A
B
C
D
E
1 mm
F
G
H
I
J
K

smaller by one-third to one-half, while having slightly shorter thecae. However, other parameters do not differ (the number of thecae is the same and the sicula is also significantly larger compared to other species of *Parapetalolithus*) with the occurrence of both subspecies restricted in the Czech Republic to the *linnaei* Biozone (*P. elongatus* has been recorded also from the upper Aeronian *halli* Biozone in Spain; Loydell *et al.* 2015).

In this study, these subspecies are not recognised. Following the analyses of measurements of various morphological parameters in numerous specimens, the variants are considered as belonging to a single species: *P. elongatus*. A similar conclusion was reached by Schauer (1971). Loydell (1992) disagreed and considered *P. linearis* to be a separate species (see also Loydell *et al*. 2015). He argued that Schauer's work was based on tectonically affected material. However, the Želkovice material studied herein is not tectonically affected. *Parapetalolithus elongatus* has been widely recorded. In the deep marine strata of the Welsh Basin, Great Britain, it is quite rare (Loydell 1992). Gutiérrez-Marco & Štorch (1998) recovered *P. elongatus* from the *palmeus* and *hispanicus* subzones in Spain. Štorch & Kraft (2009) documented *P. elongatus* from the Mrákotín Formation (Hlinsko Zone of the Bohemian Massif). Chen (1984) recorded the species from China. Williams *et al.* (2016) mentioned the occurrence of *Parapetalolithus elongatus* (Bouček & Přibyl), along with *Parapetalolithus conicus* (Bouček) [= *hispanicus*], and *Parapetalolithus giganteus* (Bouček & Přibyl), from the *Pristiograptus renaudi* Subzone (a subdivision of the *Spirograptus guerichi* Biozone) in Saudi Arabia.

***Parapetalolithus ovatus* (Barrande, 1850)**
Figures 4F; 8A–N; 13A–C

1850 *Graptolithus ovatus*; Barrande, pp. 63–64, pl. 3, figs 8, 9.
1851 *Graptolithus ovatus* Suess. – Suess, pp. 105–106, pl. 8, fig. 3.
1908 *Petalograptus* cf. *ovatus* Elles & Wood. – Elles & Wood, p. 278, pl. 32, fig. 6, text-fig. 192.
1941a *Petalolithus ovatus* Suess, 1851. – Bouček & Přibyl, pp. 18–20, text-fig. 1, figs 8–9, pl. 1, figs 8–10.
1992 *Petalolithus ovatus* (Barrande, 1850). – Loydell, pp. 46–47, pl. 2, fig. 8, text-fig. 13, fig. 10 (see for further synonymy).
2008 *Parapetalolithus ovatus* (Barrande, 1850). – Štorch *in* Zalasiewicz & Rushton, fig. 2.63.
2009 *Parapetalolithus ovatus* (Barrande, 1850). – Štorch & Kraft, p. 66, figs 7c, 10b.
2021 *Parapetalolithus ovatus* (Barrande, 1850). – Hopfensperger *et al*., fig. 3l.

Lectotype. – Figured herein (Fig. 4F), designated by Bouček & Přibyl (1941a, p. 14), Figured by Barrande (1850, pl. 3, fig. 8) and Bouček & Přibyl (1941a, pl. 1, fig. 9). Specimen NML 27579 from Želkovice, Bohemia.

Material. – Sixty specimens from the middle *linnaei* Biozone from Želkovice near Libomyšl.

Diagnosis. – Oval rhabdosome is typical. Dorso-ventral width increases significantly in the proximal part, but decreases in a similar manner at the distal end. Sicula is long (1.16–1.65 mm), sicular apex attains the level of the 3rd–4th thecal pair. Thecae are concave to the proximal end, having curved ventral walls and everted apertures. The inclination of some proximal apertures can almost be parallel to the axis of rhabdosome. Thecae overlap for four-fifths to five-sixths of their length. Angle of divergence on the 3rd thecal pair varies from 85–110°.

Description. – Rhabdosome is oval and relatively short, 4.2–5.5 mm (exceptionally 7 mm) long. Sicula length reaches 1.16–1.6 mm. Width of the sicula aperture is 0.2–0.4 mm. Length of the free part of the dorsal wall of the sicula is 0.25–0.53 mm, most frequently 0.4–0.5 mm. Apex of sicula reaches the 3rd–4th thecal pair in adult specimens, but reaches only the 2nd and 3rd thecal pair in juveniles. Curvature of the ventral thecal walls of the 1st thecal pair is very considerable. Apical angle measured on the 1st pair of thecae ranges from 143° to 178°, mostly 150–170°. Angle of divergence (AD – Fig. 3) on the 1st pair of thecae ranges between 68.5–120°, on the 3rd thecal pair the between 85 and 110° and then, on the 5th and 6th thecal pairs decreases to 80–110° and 58.6–96° respectively. Angle of apertures (AP – Fig. 3) reaches 45–117° between the 5th and 6th thecal pair and 28–103° at the 6th and 7th thecal pairs.

Dorso-ventral width (abbreviated DVW) is very variable, reflecting the gradual growth of the colony and its typical oval to almost circular rhabdosome shape. Initially, DVW increases continuously: measured values for th1 are 1.57–2.07 mm, at th3 2.55–3.79 mm, at th5 2.72–4.95 mm and 2.89–4.93 mm at the 6th thecal pair. DVW reaches its maximum between the 6th–8th thecal pairs and then DVW begins to decrease gradually. The following values

Figure 7. The astogeny of *Parapetalolithus elongatus* (Bouček & Přibyl, 1941a) from the juvenile stage (Figs A–H) to the adult stage. A – ZAZ 28; B – ZAZ 29; C – ZAZ 30; D – ZAZ 31; E – ZAZ 32; F – ZAZ 33; G – ZAZ 34; H – ZAZ 35; I – PŠ 469/2; J – ZAZ 36; K – ZAZ 37; L – ZAZ 38; M – ZAZ 39; N – PŠ 470; O – ZAZ 40. All specimens originate from the *linnaei* Biozone, lowermost Litohlavy Formation, Želkovice. Scale bars represent 1 mm.

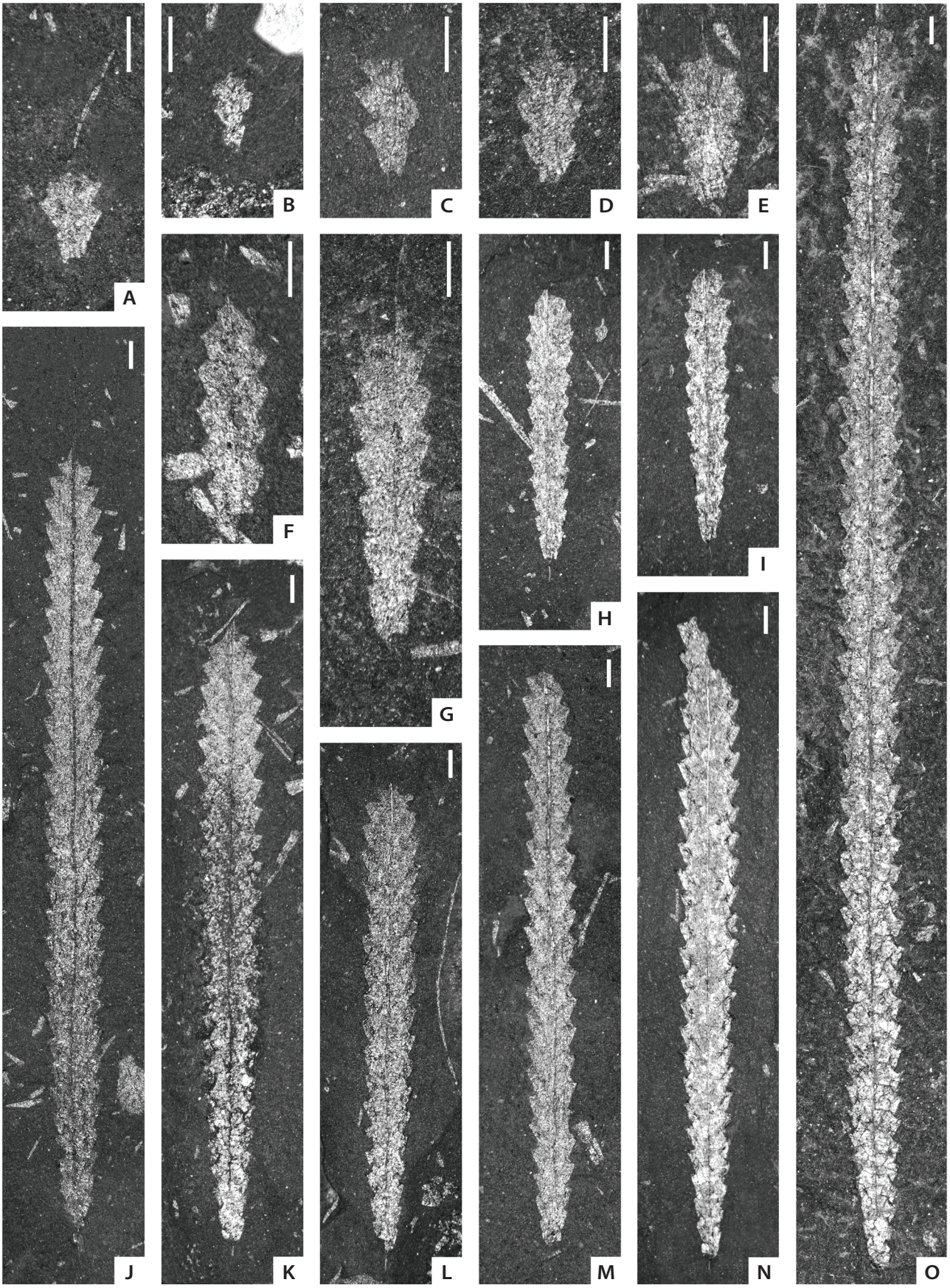
A
B
C
D
E
F
G
H
I
J
K
L
M
N
O

were measured for the most mature (gerontic) specimens (with 10 and more thecae): the width decreases to 2.33–5.06 mm at the 8th thecal pair and 2.35–4.06 mm at the 10th thecal pair. The width of apertures is relatively constant and increases only very slightly in the distal thecae. Average values are 0.27–0.62 mm at the 1st thecal pair, 0.26–0.75 mm at the 2nd thecal pair, 0.28–0.76 mm at the 3rd thecal pair, 0.21–0.93 mm at the 5th thecal pair and 0.35–0.94 at the 7th thecal pair. Thecae overlap relatively consistently by four-fifths to five-sixths of their length in the proximal part of the rhabdosome. The $2TRD_2$ values are 0.52–1.19 mm, while $2TRD_5$ and $2TRD_{10}$ values are 0.60–1.65 mm and 1.16–1.69 mm, respectively. At the distal end of the rhabdosome, two pairs of incomplete thecae were commonly observed; occasionally, three pairs (see Fig. 8B–D). A twisted ribbon-like nema structure or straight ribbon-like nematularium were observed in some specimens (see Fig. 6B).

The early juveniles of *P. ovatus* are easily recognisable (compared to juveniles of *P. palmeus*, *P. hispanicus* or *P. elongatus*) due to the atypically high values of DVW and AD (described above) already at 1th–5th thecal pair. First thecal pairs grow almost perpendicularly to the sicula, as can be seen in the Fig. 8A–G. Angle of divergence differs very little between juveniles and adults. The deviation AD on each thecal pair is about 2–3 degrees.

Discussion. – This well-recognisable species was first described by Barrande (1850). According to Bouček & Přibyl (1941a), it is a common species in the Prague Basin. Its occurrence is limited to the *linnaei* Biozone in the Czech Republic. Compared with other species of *Parapetalolithus*, *P. ovatus* is wider and has a notably shorter rhabdosome. *P. ovatus* has been described also from Wales (Loydell 1992) where a single specimen was described from the upper Aeronian *halli* Biozone, and southwestern Sardinia (Štorch & Piras 2009).

There are no documented specimens of *P. ovatus* from Spain, neither from Sierra Morena (Haberfelner 1931) nor from the El Pintado reservoir (Loydell *et al*. 2015). However, a similar species, *Parapetalolithus regius* (Hundt), is reported from Spain (Loydell *et al*. 2015). *P. ovatus* is often compared with the following two species*: Parapetalolithus globosus* (Chen) and *Parapetalolithus regius* (Hundt).

Parapetalolithus globosus (Chen, 1984) exhibits a narrower rhabdosome than *P. ovatus*. This species has been recently reported from the Tielugou section in China by Maletz *et al*. (2021). *Parapetalolithus regius* (Hundt, 1957) has a maximum rhabdosome width comparable to *P. ovatus*. Nevertheless, it has a notably different angle of divergence on the proximal part of the rhabdosome and a different inclination of thecal apertures relative to the rhabdosome axis. These differences are well discernible in the illustrations of many authors (*e.g*. Hundt 1957, Loydell 1992, Štorch & Kraft 2009, Loydell *et al.* 2015, Maletz *et al*. 2021). Štorch & Kraft (2009) documented both species – *P. ovatus* (Barrande) and *P. regius* (Hundt) – from the Mrákotín Formation (Hlinsko Zone of the Bohemian Massif). Although this is tectonically deformed material, the differences between the two species outlined above are still clearly visible.

***Parapetalolithus hispanicus* (Haberfelner, 1931)**
Figures 4G; 9A–N; 13D, L, N, P

1923 *Diplograptus* (*Petalograptus*) *altissimus* Elles & Wood. – Gortani, p. 5, pl. 1, fig. 6.
1931 *Petalograptus hispanicus* nov. sp.; Haberfelner, pp. 49–50, pl. 1, figs 11a–d.
1932 *Petalograptus conicus* n. sp.; Bouček, pp. 151–154, text-fig. 2a, b.
1941a *Petalograptus hispanicus* (Haberfelner 1931). – Bouček & Přibyl, pp. 14–15, pl. 2, fig. 5, text-fig. 2, figs 16–19.
1941a *Petalograptus conicus* (Bouček, 1932). – Bouček & Přibyl, pp. 15–16, pl. 2, fig. 4, text-fig. 2, figs 9, 10.
1992 *Petalolithus conicus* (Bouček, 1932). – Loydell, pp. 39–40, pl. 2, fig. 1; text-fig. 12, figs 8, 18–21.
1992 *Petalolithus hispanicus* (Haberfelner, 1931). – Loydell, pp. 44–45, text-fig. 12, figs 1–2 (see for further synonymy).
1998 *Parapetalolithus hispanicus* (Haberfelner). – Gutiérrez-Marco & Štorch, fig. 8r.
1998 *Parapetalolithus hispanicus* (Haberfelner). – Štorch, pl. 1, fig. 6, text-fig. 3, fig. 2.
2000 *Petalolithus conicus* (Bouček). – Štorch *in* Zalasiewicz *et al*., fig. 1.73.
2003 *Parapetalolithus* cf. *hispanicus* (Haberfelner). – Štorch & Massa, figs 5, 16.
2015 *Parapetalolithus hispanicus* (Haberfelner). – Loydell *et al*., figs 16ag, 18y.
2018 *P. conicus* (Bouček, 1932). – Lenz *et al*., p. 10, fig. 8.3c.

Lectotype. – Subsequently designated by Přibyl (1948, p. 13), Figured by Haberfelner (1931, pl. 1, fig. 11a) from the *linnaei* Biozone of Almaden, Sierra Morena, Spain.

Figure 8. The astogeny of *Parapetalolithus ovatus* (Barrande, 1850) from the juvenile stage (Figs A–E) to the adult stage. A – ZAZ 41; B – ZAZ 42; C – ZAZ 43; D – ZAZ 44; E – ZAZ 45; F – ZAZ 46; G – PŠ 474/1; H – ZAZ 47; I – ZAZ 48; J – PŠ 474/2; K – ZAZ 49; L – ZAZ 50; M – ZAZ 51; N – ZAZ 52. All specimens originate from the *linnaei* Biozone, lowermost Litohlavy Formation, Želkovice. Scale bars represent 1 mm.

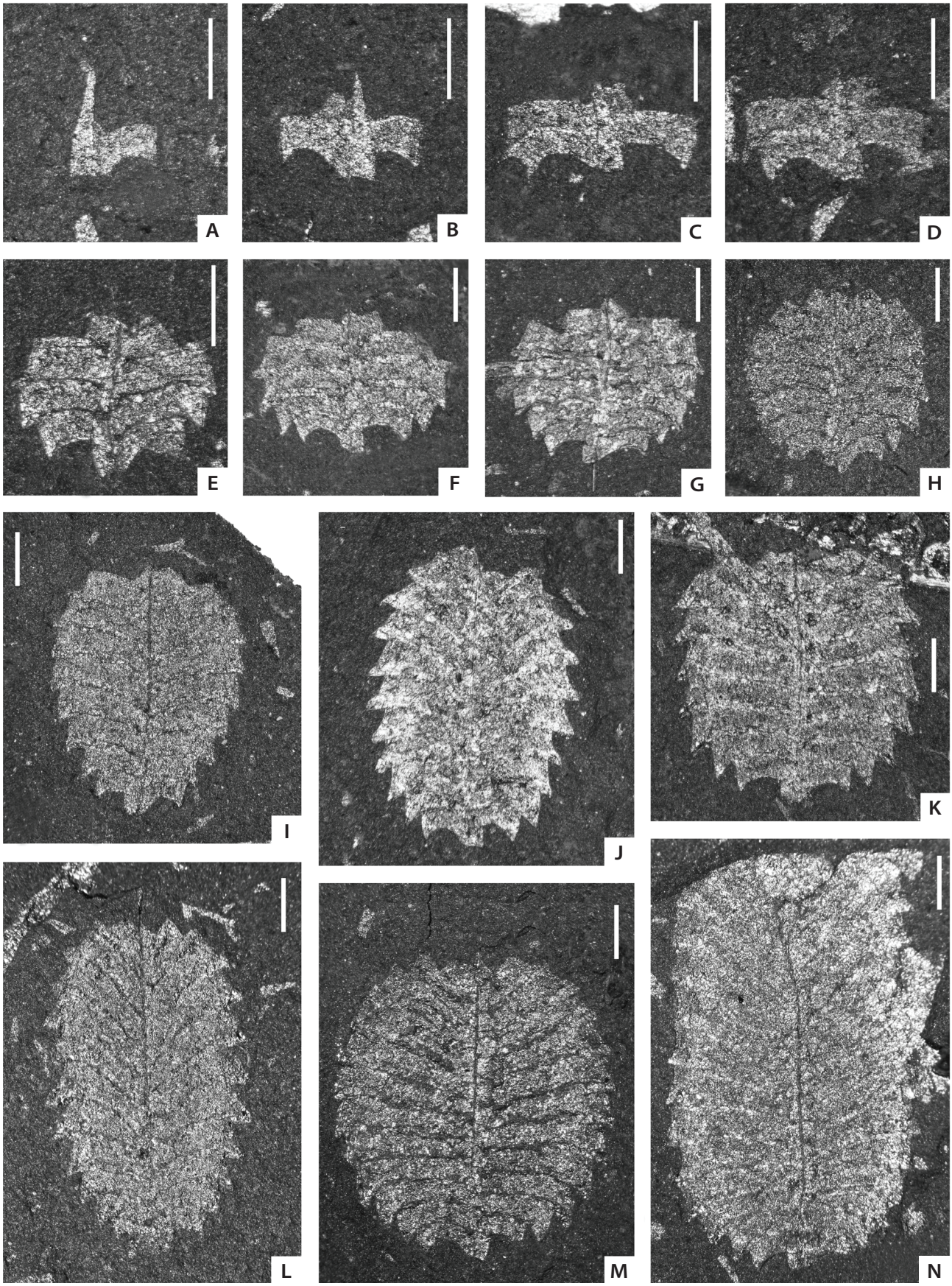
A
B
C
D
E
F
G
H
I
J
K
L
M
N

Material. – Four hundred and eighteen specimens from the upper *linnaei* Biozone of Želkovice near Libomyšl.

Diagnosis. – Robust rhabdosome with a V-shaped proximal part. The conspicuously widening proximal part reaches its maximum dorso-ventral width (*ca*. 3 mm) around the 10th thecal pair and remains constant thereafter. Sicula is small, 0.96–1.33 mm long and its apex attains the level of the 2nd thecal pair. Thecae are simple tubes and thecal apertures are straight. Angle of divergence on the 3rd thecal pair ranges between 32–53°.

Description. – Rhabdosome is robust, with markedly tapering proximal portion, usually about 20 mm long. The sicula reaches 1.0–1.33 mm long. The most common measured values were 1.26 and 1.31 mm. Width of the sicula aperture fluctuates between 0.19–0.35 mm. Length of the free part of the dorsal wall of the sicula varies from 0.42 to 0.62 mm. Sicular apex attains the level of the 2nd thecal pair in adult specimens, but reaches the 2nd–3rd thecal pair in juveniles. Curvature of the ventral thecal walls of the 1st thecal pair is very slight. Apical angle measured at the 1st thecal pair ranges from 62° up to 95°, but usually between 70–80°. Angle of divergence (AD – Fig. 3) does not change significantly. On the 1st thecal pair, the angle ranges from 29–52°, on the 3rd thecal pair 40–52° and on the 5th and 6th thecal pairs decreases to 33–49° and 33–48° respectively. Angle of apertures (AP – Fig. 3) reaches 76–117° between the 5th and 6th thecal pairs and 70–112° between the 6th and 7th thecal pairs. Dorso-ventral width (DVW) increases continuously without larger fluctuations. The measured values of DVW for th1 are 0.72–1.30 mm, for th3 1.32–1.89 mm, for th5 1.71–2.36 mm and at th6 DVW reaches 1.61–2.59 mm. The most mature specimens (with 10 or more thecae) have DVW values at th8 and th10 of 2.08–3.08 mm and 2.01–3.38 mm, respectively. The width of apertures increases very slightly, but continuously, distally. They are 0.19–0.39 mm wide at the 1st thecal pair, 0.19–0.45 mm at the 2nd thecal pair, 0.28–0.57 mm at the 3rd thecal pair, 0.24–0.67 mm at the 5th thecal pair and 0.35–0.87 at the 7th thecal pair. Thecae overlap by one half their length in the proximal part of the rhabdosome and by one half to two-thirds their length in the distal part of the rhabdosome. The values of $2TRD_2$ are 0.99–1.60 mm, while $2TRD_5$ and $2TRD_{10}$ values range between 1.29–1.67 mm and 1.17–1.82 mm, respectively. At the distal end of the rhabdosome, two unfinished pairs of thecae were commonly observed.

A nematularium was observed as a long, parallel-sided or spirally twisted ribbon, slightly widening distalwards in some specimens (Fig. 6A, D).

The early juveniles of *P. hispanicus* are well-recognisable due to the conspicuously widening proximal part of the rhabdosome and relatively constant AD, regardless of whether the measured specimen is a juvenile or mature stage. Thanks to this, the early stages of *hispanicus* juveniles (especially, from 3th–5th thecal pair) may resemble an inverted "isosceles triangle" (see Fig. 9C–F).

Discussion. – *Parapetalolithus hispanicus* was first described from Spain by Haberfelner (1931). Bouček (1932) established a very similar species, *Petalolithus conicus*, in the Prague Synform. Later, Bouček & Přibyl (1941a) re-classified most of the specimens originally designated as *P. conicus* to *P. hispanicus*. However, the holotype of the species *P. conicus* (Fig. 4G) and an unspecified number of specimens remained valid, with *P. conicus* being described as a rare species. They distinguished *P. conicus* from *P. hispanicus* based on a stronger virgula (nema) and a higher number of thecae in 10 mm (*P. conicus* having 13–14 thecae, *P. hispanicus* 11–12 thecae). In this study, specimens of possible *P. conicus* lie within the intraspecific variability of *P. hispanicus*. *P. conicus* can thus be considered a junior synonym of *P. hispanicus*, confirming the conclusions of Štorch (1998). Gutiérrez-Marco & Štorch (1998) recorded *P. hispanicus* from shelf deposits of the Western Iberian Cordillera in Spain, where they recognised a *hispanicus* Subzone, yielding *Parapetalolithus hispanicus* (Haberfelner), *P. elongatus* (Bouček & Přibyl) and *P*. cf. *altissimus* (Elles & Wood). Some specimens of *P. hispanicus* were documented in Libya (Štorch & Massa 2003). Furthermore, Štorch & Piras (2009) mentioned the occurrence of *P. hispanicus*, *P. ovatus*, *P. elongatus* and *P*. cf. *hispanicus* from the *linnaei* Biozone in Sardinia.

Loydell *et al.* (2015) described *Parapetalolithus elizabethae*, from the El Pintado reservoir near Sevilla, Spain (illustrated in their figs 16e, 18ad), established on the basis of three diagenetically flattened specimens, two from the lower *halli* Biozone (upper Aeronian) and one from the middle *guerichi* Biozone, which are highly similar to *P. hispanicus*. The species were stated to be distinguished based on the width of rhabdosome in the distal part, a slightly different shape of the proximal end, and the angle of inclination of thecae. Until the species are subjected to a highly detailed comparison based on larger collection of *P. elizabethae*, the latter cannot be marked as a junior

Figure 9. The astogeny of *Parapetalolithus hispanicus* (Haberfelner, 1931) from the juvenile stage (Figs A–I) to the adult stage. A – ZAZ 15; B – ZAZ 16; C – ZAZ 17; D – ZAZ 18; E – ZAZ 19; F – ZAZ 20; G – ZAZ 21; H – ZAZ 22; I – ZAZ 23; J – ZAZ 24; K – PŠ 244; L – ZAZ 25; M – ZAZ 26; N – ZAZ 27. All specimens originate from the *linnaei* Biozone (*hispanicus* Subzone), lowermost Litohlavy Formation, Želkovice. Scale bars represent 1 mm.

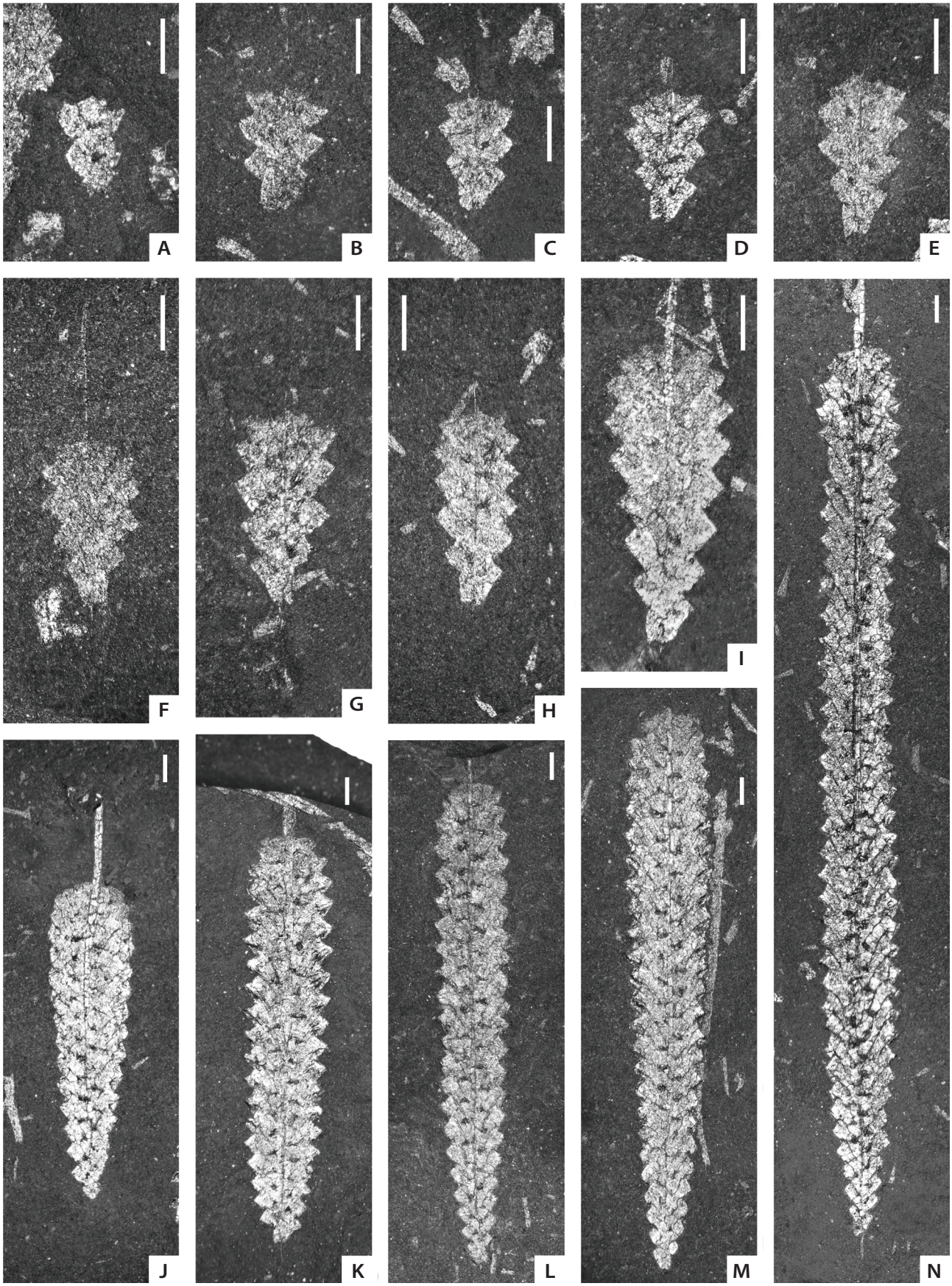
A
B
C
D
E
F
G
H
I
J
K
L
M
N

synonym of *P. hispanicus*. If it was, the stratigraphical range of *P. hispanicus* would be extended considerably. Loydell *et al.* (2015) distinguished *P. fusiformis* (Chen, 1984) from *P. elongatus* based on "*Pa. fusiformis* differs from *Pa. elongatus* (Bouček & Přibyl, 1941a; figs 16ad, 18ap) in its more rapidly increasing rhabdosome width proximally and conspicuously fusiform rhabdosome outline". However, the general shape of the rhabdosomes, as well as the increasing dorso-ventral width in the two illustrated specimens, somewhat resemble *P. hispanicus*. Maletz *et al*. (2021) recorded *P. fusiformis* from the Tielugou section in China; the specimen illustrated (fig. 13g, i) resembles *P. hispanicus*.

***Parapetalolithus altissimus* (Elles & Wood, 1908)**
Figures 4B; 10A–G; 11A; 13F, H, I

partim	1908	*Petalograptus altissimus* sp. nov.; Elles & Wood, pp. 281–282, pl. 32, figs 7a, e (*non* b–d), text-fig. 194c (*non* a, b).
	1941a	*Petalograptus altissimus* Elles & Wood 1908. – Bouček & Přibyl, pp. 16–17, text-fig. 3, figs 4–7.
	1992	*Petalolithus altissimus* (Elles & Wood, 1908). – Loydell, pp. 36–39, text-fig. 12, figs 7, 16, 17 (see for further synonymy).
	2003	*Parapetalolithus altissimus* (Elles & Wood). – Loydell *et al*., fig. 6j.
	2010	*Parapetalolithus altissimus* (Elles & Wood). – Loydell *et al*., p. 254, fig. 2o.
	2015	*Parapetalolithus altissimus* (Elles & Wood). – Loydell *et al*., fig. 16ae.
	2016	*Parapetalolithus altissimus* (Elles & Wood). – Williams *et al*., fig. 8g.
	2017	*Parapetalolithus latissimus.* – Loydell *et al*., fig. 16a.
	2017	*Parapetalolithus altissimus* (Elles & Wood). – Suyarkova, fig. 23ž.

Lectotype. – Figured herein (Fig. 4B), designated by Přibyl (1948, p. 12). Specimen GSE 5622 from the Upper Birkhill Shales of Black Linn, Glenkiln Burn, Strathclyde, Scotland, figured by Elles & Wood (1908, pl. 32, fig. 7a).

Material. – Seven specimens from the upper *turriculatus* and *crispus* biozones from Litohlavy near Králův Dvůr.

Diagnosis. – Rhabdosome is robust (around 3 mm wide) with significant widening in the proximal part of the rhabdosome. Sicula is small, with maximum length of 1.32 mm and its apex attains the base of the 2nd thecal pair. Thecae are simple tubes; thecal apertures are straight or can be everted slightly. The thecae are widely spaced. The thecal overlap varies from two-thirds to three-quarters of their length. Angle of divergence of the 3rd thecal pair reaches 38–45° and then remains relatively constant.

Description. – Rhabdosome is robust, 25–30 mm long, with markedly tapering proximal part. Sicula length reaches 1.12–1.32 mm. Width of the sicula aperture is 0.21–0.36 mm. Length of the free part of the dorsal wall of the sicula varies from 0.33 to 0.45 mm. Apex of sicula seems to attain the 2nd thecal pair in adult specimens, but it reaches up to the 3rd thecal pair in juvenile specimens. Apical angle measured at the 1st thecal pair ranges from 53° to 86°. Ventral thecal walls of the 1st thecal pair are essentially straight. Angle of divergence (AD – Fig. 3) increases slightly proximally and then remains relatively constant. On the 1st thecal pair, the angle ranges between 26–46°, on the 3rd thecal pair 38–45°, at the 5th pair 33–55° and at the 6th pair thecal pair 37–55°. Angle of apertures (AP – Fig. 3) is 92–117° between the 5th and 6th thecal pair and 85–125° between the 6th and 7th thecal pair. Dorso-ventral width (DVW) shows a gradual increase up to the 5th thecal pair; the values of DVW stagnate afterwards. Values at th1 are 1.00–1.52 mm, at th3 1.57–2.42 mm, at th5 1.90–2.95 mm and at th6 2.49–3.07 mm, respectively.

In the most mature specimens (with 10 or more thecae), DVW values increase continually up to the 8th and 10th thecal pairs (to 2.92–3.06 mm and 2.83–3.26 mm, respectively).

The width of apertures increases very slightly. Its values are 0.21–0.55 mm at the 1st thecal pair, 0.24–0.58 mm at the 3rd thecal pair, 0.26–0.59 mm at the 5th thecal pair and 0.36–0.66 mm at the 7th thecal pair. Thecal overlap is two-thirds of thecal length in juvenile stages and three-quarters of thecal length in the distal part of adult specimens. The $2TRD_2$ values are 1.03–1.68 mm, while $2TRD_5$ and $2TRD_{10}$ values range between 1.07–1.77 mm and 1.82–2.71 mm, respectively. At the distal end of the rhabdosome, two pairs of incomplete thecae were commonly observed; occasionally, three pairs of incomplete thecae were noted in juvenile stages (Fig. 10B, C). A twisted ribbon-like nematularium was observed in some specimens (Fig. 6K), clearly bifurcated in one specimen (see Figs 10C, 13F).

Juveniles of *P. altissimus* are characteristic by rapidly expanding first pairs of thecae and relatively constant AD values. The combination of these two parameters (DVW and AD) gives the shape, which is best visible at the juvenile stages of 3th–5th thecal pairs (see Fig. 10A, B).

Discussion. – *Parapetalolithus altissimus* was first described by Elles & Wood (1908) from Great Britain. In the Prague Basin, it is documented from the *turriculatus*, *crispus* and *griestoniensis* biozones (Bouček & Přibyl, 1941a). It differs from *P. palmeus* in the angle of divergence and DVW (see Table 1) and it has shorter and

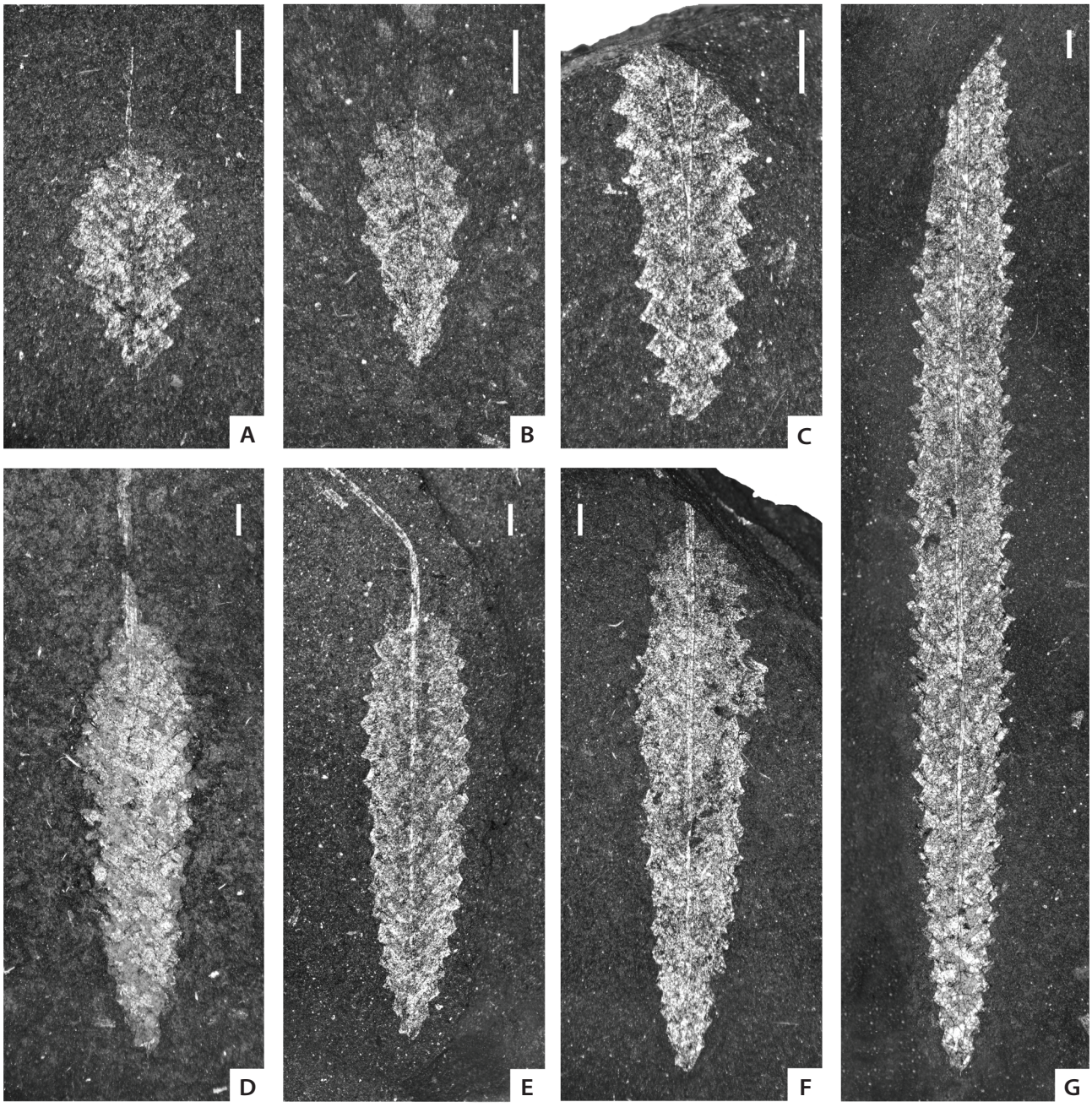

Figure 10. The astogeny of *Parapetalolithus altissimus* (Elles & Wood, 1908) from the juvenile stage (Figs A–C) to the adult stage. A – ZAZ 53; B – ZAZ 54; C – ZAZ 55; D – ZAZ 56; E – ZAZ 57; F – ZAZ 58; G – ZAZ 59. All specimens originate from the lower *crispus* Biozone, Litohlavy Formation, Litohlavy near Králův Dvůr. Scale bars represent 1 mm.

less overlapping most proximal thecae. *Parapetalolithus altissimus* is similar to *P. hispanicus* in having a very similar angle of divergence, but *P. altissimus* is more robust. Due to their similarity and the fact that they occur in successive biozones, Bouček & Přibyl (1941a) proposed that *P. altissimus* may have been an evolutionary successor of *P. hispanicus*. However, the type material of *P. altissimus* is from the upper Aeronian and the species appears in the *guerichi* Biozone in Spain (Loydell *et al*. 2015).

Parapetalolithus giganteus (Bouček & Přibyl, 1941a) is known not only from Germany (Bouček & Přibyl 1941a), but also from Wales (Loydell 1992) and Saudi Arabia (Williams *et al*. 2016). All authors mention its occurrence within black shales corresponding to the lower Telychian *R. linnaei* or *S. guerichi* Biozone. According to Bouček & Přibyl (1941a) it differs from *P. altissimus* (and other species) by the larger size of the rhabdosome and greater number of thecae in 10 mm (12–15 thecae).

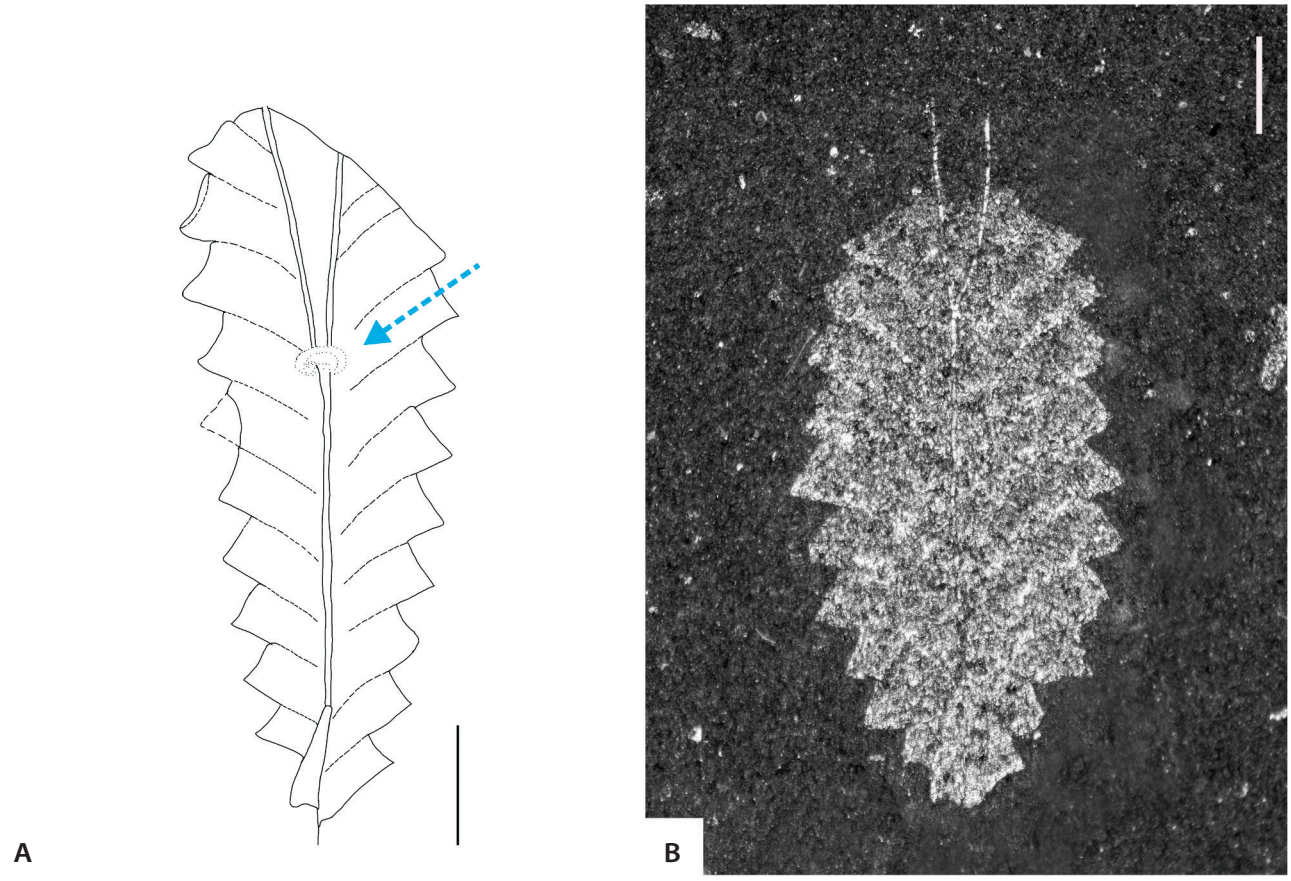

Figure 11. A – *Parapetalolithus altissimus* (Elles & Wood, 1908), ZAZ 55; specimen with a bifurcated nematularium. The blue arrow shows the origin of a bifurcated nematularium and an unusual, ring-shaped object, possibly of parasitic origin. • B – *Parapetalolithus* cf. *altissimus*, PŠ 240; apparently an aberrant specimen of *P. altissimus*, first published by Štorch (1992) as *Petalolithus* sp. Both specimens originate from the *turriculatus* Biozone, Litohlavy Formation, Litohlavy near Králův Dvůr.

However, the sicula was not preserved. Bouček & Přibyl (1941a) admitted the possibility that the width of the largest specimens may have been caused by deformation. The type specimen of *P. giganteus* is highly compressed and tectonically enlarged (Zalasiewicz *et al*. 2000, p. 74) and the species should be regarded as a junior synonym of *P. altissimus* as suggested by Štorch (1998, p. 118).

Loydell *et al*. (2003) recorded *P. altissimus* and *P. schaueri* from the Aizpute-41 core in Latvia. Their illustrations include a specimen with a bifurcated nematularium, which was also observed in two specimens in Bohemia (Fig. 11A, B). The question of its origin is not clear – the possibility of parasitism cannot be excluded. In one of the studied specimens, where the nematularium bifurcates, at the same level, there is an unusual, ring-shaped object (Fig. 11A).

However, such a ring-shaped object was not observed in other specimens and is not mentioned or drawn in other works either. On the other hand, finding, recognising and proving parasitism in graptolites is not easy, as evidenced by the works of Underwood (1993), Bates & Loydell (2000), Muir (2011) and Taylor (2015). However, Muir (2011) described a bifurcated nematularium in *Glyptograptus* and in the controversy over its origin mentions the possibility of a genetic abnormality or damage to the rhabdosome during life.

Štorch (1992) found one unusual specimen of *Parapetalolithus* (Fig. 11B) in the uppermost *Spirograptus turriculatus* Biozone from Litohlavy near Králův Dvůr. He pointed out its bifurcated nematularium and discusses its similarities to *P. palmeus* and *P. ovatus* based on morphometric data (rhabdosome shape, dimensions and thecal inclination). In this study, this specimen is referred to *P*. cf. *altissimus* (Fig. 11B). Apparently, this is an aberrant specimen. *P. altissimus* is present in several countries. Gutiérrez-Marco & Štorch (1998) mentioned its possible occurrence in Spain, similarly to *P.* cf. *altissimus*, but they described it from the *hispanicus* Subzone, which is somewhat unusual because its first appearance is in the *turriculatus* Biozone in the Prague Basin. Further, Štorch & Piras (2009) noted *P. altissimus* and other species of *Parapetalolithus* from southwestern Sardinia.

Loydell *et al.* (2010) recorded *P. altissimus* from the Kolka-54 core in Latvia. Loydell *et al*. (2017) identified *P. tenuis* (Barrande) and *P. altissimus* (Elles & Wood) from Bornholm in the Sommerodde-1 core (in the *turriculatus* Biozone) and Suyarkova (2017) documented *P. altissimus* from the Kaliningrad District in the *turriculatus* and *crispus* biozones.

***Parapetalolithus tenuis* (Barrande, 1850)**
Figures 4C; 12A–M; 13E, G

partim 1850	*Grapt. palmeus Barrande* Var. *tenuis*; Barrande, pp. 59–63, pl. 3, fig. 2 (*non* 1).
partim 1851	*Petalolithus palmeus.* – Suess, pp. 104–105, pl. 8, fig. 1a (*non* b, c).
partim 1897	*Diplograptus palmeus* varianta *tenuis* Barrande. – Perner, p. 3, pl. 9, figs 3, 7 (5, *non* 6).
non 1908	*Petalograptus palmeus* varianta *tenuis*, Barrande. – Elles & Wood, pp. 276–277, pl. 32, figs 3a–d, text-fig. 190.
1941a	*Petalolithus tenuis* (Barrande 1850). – Bouček & Přibyl, pp. 9–10, pl. 2, fig. 3, text-fig. 2, figs 8–11.
1992	*Petalolithus tenuis* (Barrande, 1850). – Loydell, pp. 53–54, pl. 1, fig. 9, text-fig. 13, figs 7, 11, 12, 18, 23 (see for further synonymy).
2000	*Parapetalolithus tenuis* (Barrande). – Štorch *in* Zalasiewicz *et al*., fig. 1.72.
2009	*Parapetalolithus tenuis* (Barrande). – Štorch & Kraft, p. 58, pl. 2, fig. 10c.
2015	*Parapetalolithus tenuis* (Barrande). – Loydell *et al*., fig. 18aj.
2017	*Parapetalolithus tenuis* (Barrande). – Loydell *et al*., fig. 14m.

Lectotype. – Figured herein (Fig. 4C), designated by Bouček & Přibyl (1941a, p. 7). Specimen NML 27569 from Litohlavy near Králův Dvůr, Bohemia, figured by Barrande (1850, pl. 3, fig. 2).

Material. – Thirty-two specimens from the upper *turriculatus* and *crispus* biozones of Litohlavy near Králův Dvůr.

Diagnosis. – Comparatively narrow rhabdosome with almost constant width 1.7–2.3 mm in the proximal and distal part of rhabdosome. Sicula is relatively long (the maximum measured value is 1.72 mm) and sicular apex attains the level of the 2nd–3rd thecal pair. Thecae are simple tubes, with slightly curved apertures. Angle of divergence on the 3rd pair of thecae ranges between 26–51°.

Description. – Rhabdosome is narrow, 16.6–19.7 mm long. Sicula length is 1.21–1.72 mm. Width of the sicula aperture varies between 0.22–0.41 mm. Length of the free part of the dorsal wall of the sicula is 0.25 to 0.59 mm. Apex of sicula attains the 2nd–3rd pair of thecae. Curvature of the ventral thecal walls of the 1st thecal pair is imperceptible. Apical angle measured at the 1st thecal pair ranges from 38° to 77°, usually 40–56°. Angle of divergence (AD – Fig. 3) increases gradually to the 5th pair of thecae, after which AD stays constant or decreases very slightly. On the 1st thecal pair, it is 22–35°, on the 3rd thecal pair, 26–47°, on the 5th thecal pair 24–45°, decreasing to 22–47° for the 6th thecal pair. Angle of apertures (AP – Fig. 3) reaches 94–127° between the 5th and 6th thecal pairs and 98–127° between the 6th and 7th thecal pairs.

Dorso-ventral width (DVW – Fig. 3) increases gradually to the 5th thecal pair (exceptionally to the 7th thecal pair) and then increases only very slightly. For th1, DVW it is 0.95–1.46 mm, at th3 1.38–2.00 mm, at th5 1.63–2.31 mm and at th7 1.59–2.35 mm. Distally, DVW is slightly reduced and constant. The following values were measured from mature specimens (with 10 or more thecae): 8th thecal pair, 1.6–2.3 mm, 10th thecal pair 1.63–2.23 mm.

The width of thecal apertures increases gradually and very slightly, but continually: 0.17–0.39 mm at the 1st thecal pair, 0.19–0.49 mm at the 2nd thecal pair, 0.22–0.60 mm at the 3rd thecal pair, 0.28–0.61 mm at the 5th thecal pair and 0.18–0.71 mm at the 7th thecal pair. Thecal overlap varies slightly, from one half to three-fifths of thecal length (see Figs 12I, M; 13E, G).

The values of $2TRD_2$ are 1.12–1.72 mm (most commonly 1.5 mm), while $2TRD_5$ and $2TRD_{10}$ values range from 1.12–1.9 mm and 1.2–2.10 mm, respectively. At the distal end of the rhabdosome, two unfinished thecal pairs were observed (Fig. 12A, F, L).

A twisted ribbon-like nematularium was observed in some specimens. Already in the early juvenile stages (3rd–5th thecal pairs), the notably small width of the rhabdosome (up to 2 mm) and the relatively sharp AD are clearly visible. The combination of these two parameters resulted in the apparent "rectangular" shape of all juveniles of *P. tenuis* (see Fig. 12 A, B).

Discussion. – This species was described by Barrande (1850) and Perner (1897) from several biozones of the Prague Basin (today corresponding to the *linnaei*, *turriculatus* and *crispus* biozones). Bouček & Přibyl (1941a) revised Barrande's and Perner's material and compared it with their own, more recently acquired specimens distinguishing two species of *Parapetalolithus* (then referred to *Petalolithus*): *P. elongatus* (from the *linnaei* Biozone, Želkovice locality) and *P. tenuis* (from the *turriculatus* and *crispus* biozones). *P. elongatus* and *P. tenuis* show only small differences in their morphology, in the proximal part of the rhabdosome (*P. tenuis* has

a smaller sicula and a higher angle of divergence – see diagnoses of both species). Due to the striking similarity of the two species and their consecutive stratigraphical occurrence, Bouček & Přibyl (1941a) suggested a possible direct evolutionary relationship between *P. elongatus* and *P. tenuis*. This study supports this idea (see Fig. 17).

In comparison to *P. altissimus*, *P. tenuis* is significantly narrower, has a longer sicula and a much lesser thecal overlap.

Hutt (1974) established, based on the material of Elles (1897) and Elles & Wood (1908), a new species, *P. wilsoni*. According to her, the main reasons for this decision were the differences in thecal spacing, nema structures, the rate of rhabdosome widening, and less everted thecal apertures when compared to *P. tenuis*. This opinion was supported by Loydell (1992), who added that *P. tenuis* is known from the *turriculatus* Biozone, while *P. wilsoni* occurs from the *crispus* to *griestoniensis* biozones.

However, in the Prague Synform, *P. tenuis* is known from both the *turriculatus* and *crispus* biozones and, especially, one of the four differentiating characters – the spirally twisted nematularium – is present also in *P. tenuis* (Fig. 13E) and also in the other *Parapetalolithus* species studied in this work. Large collections of *P. wilsoni* should be compared in detail with *P. tenuis* to be sure that *P. wilsoni* is a distinct species and not a junior synonym of *P. tenuis*. *P. tenuis* is documented from the *turriculatus* Biozone in Spain (Gutiérrez-Marco & Štorch 1998, Loydell *et al*. 2015), Wales (Loydell 1992), from the Hlinsko Zone of the Bohemian Massif (Štorch & Kraft 2009), from southwestern Sardinia (Štorch & Piras 2009) and from Bornholm in the Sommerodde-1 core (Loydell *et al*. 2017).

The impact of astogeny and intraspecific variability on taxonomic classification

The results of any systematic classification of graptolites can differ depending on which methodology is used by an author and which parameters are being emphasized. While revisiting Barrande's and Perner's material, as well as studying their own, Bouček & Přibyl (1941a) paid attention to and addressed the problem of the correct determination of graptolites and highlighted the importance of rhabdosome width (mainly in the proximal part) and the number of thecae in 10 mm. However, they admitted that these values can be distorted in tectonically deformed materials. The revised and newly found material studied for this work had the indisputable advantage of being very well-preserved despite being diagenetically flattened. Thanks to this, it was possible to revise the individual species of *Parapetalolithus*, comparing the results of all measured parameters across the species and verifying which parameters are the most important for the differentiation of the various *Parapetalolithus* species. Not surprisingly, the number of thecae in 10 mm and the 2TRD values used by previous authors proved to be complementary parameters.

In isolation, the width of the proximal part of the rhabdosome was an extremely unreliable parameter for taxonomical purposes within *Parapetalolithus* – there was, for example, often significant overlap of clusters of the clearly different (and biostratigraphically important) species *P. palmeus* and *P. hispanicus* (Fig. 14). The only exception, where it was sufficient to use DVW on individual thecal pairs for the taxonomic determination of the species, was *P. elongatus* (see Fig. 15).

The results of this study show that the best option is to compare and combine two parameters – the angle of divergence (AD) and the dorso-ventral width (DVW). The combination of these two parameters not only allowed clear distinction (or, to the contrary, synonymizing) of species but also highlights the extent of their morphological variability (Fig. 14). Moreover, the study was able to characterize individual species even at early juvenile stages (see Fig. 16) and thus, it was possible to create a unique astogenetic series for individual species.

When comparing species of *Parapetalolithus* within successive biozones (i.e. *linnaei*, *turriculatus* and *crispus*), small overlaps between species are present (Fig. 17). This seems to be supportive of an evolutionary link between individual species. Bouček & Přibyl (1941a) pointed out the considerable morphological similarity of *P. elongatus* and *P. tenuis* as well as between *P. hispanicus* and *P. altissimus* and suggested a possible ancestor–descendant relationships. The information and data obtained in this study support their opinion in the case of species *P. elongatus* and *P. tenuis* (see Fig. 17).

The systematic classification of *Parapetalolithus* is influenced not only by the methodology selected and associated choice of key parameters but also by the phenomenon of "widening" of the proximal part of the rhabdosome. This was the main reason for Bouček & Přibyl (1941a) differentiating *P. p. clavatus* from *P. p. palmeus*,

Figure 12. The astogeny of *Parapetalolithus tenuis* (Barrande, 1850) from the juvenile stage (Figs A–D) to the adult stage. A – ZAZ 60; B – ZAZ 61; C – ZAZ 62; D – PŠ 464/2; E – PŠ 458; F – ZAZ 63; G – ZAZ 64; H – PŠ 457/1; I – ZAZ 65; J – ZAZ 66; K – ZAZ 67; L – PŠ 457/2; M – ZAZ 68. All specimens originate from the uppermost *turriculatus* (4–5, 8, 12) and the lowermost *crispus* (1–3, 6–7, 9–11, 13) biozones, Litohlavy Formation, Litohlavy near Králův Dvůr. Scale bars represent 1 mm.

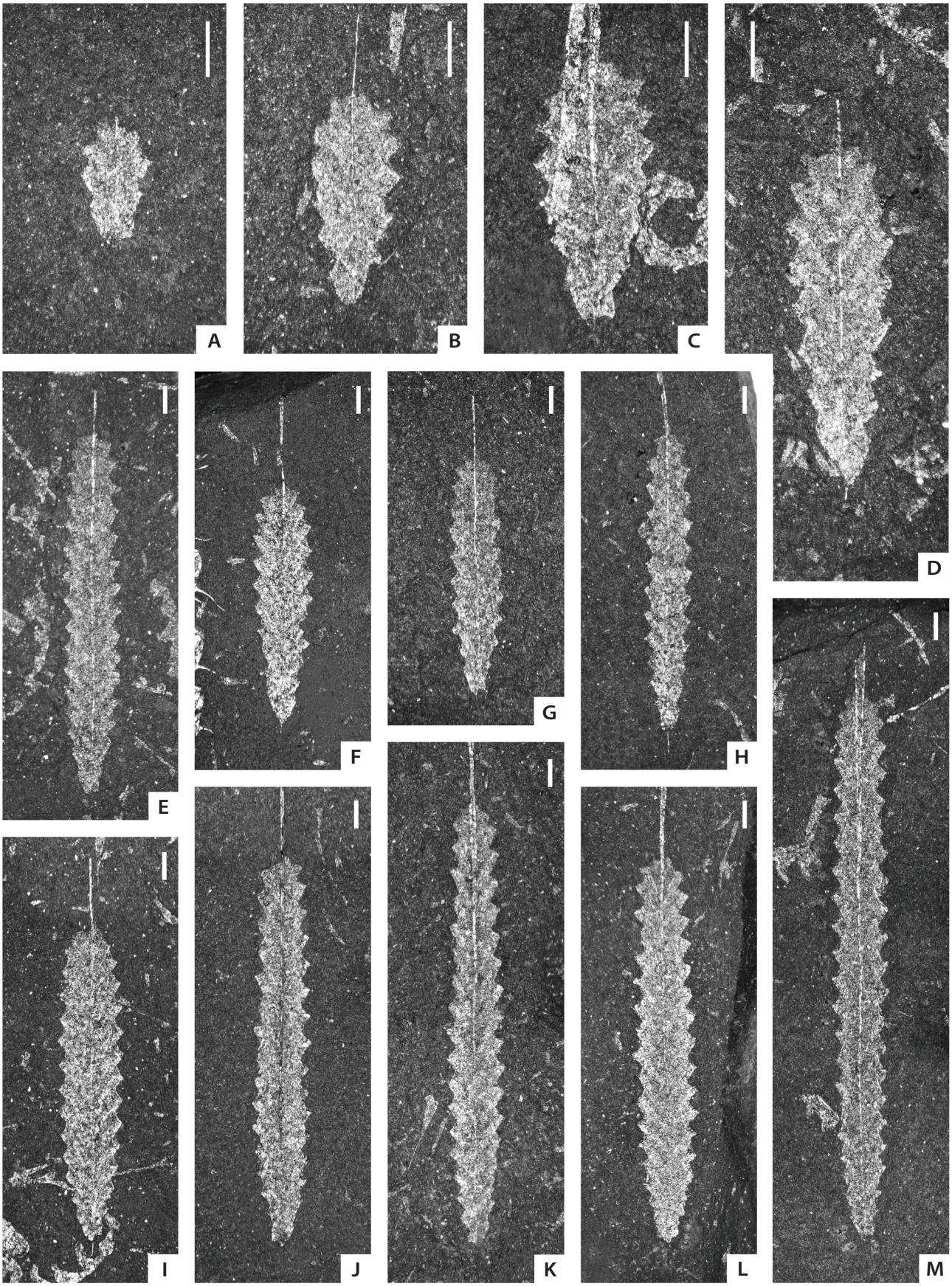
A
B
C
D
E
F
G
H
I
J
K
L
M

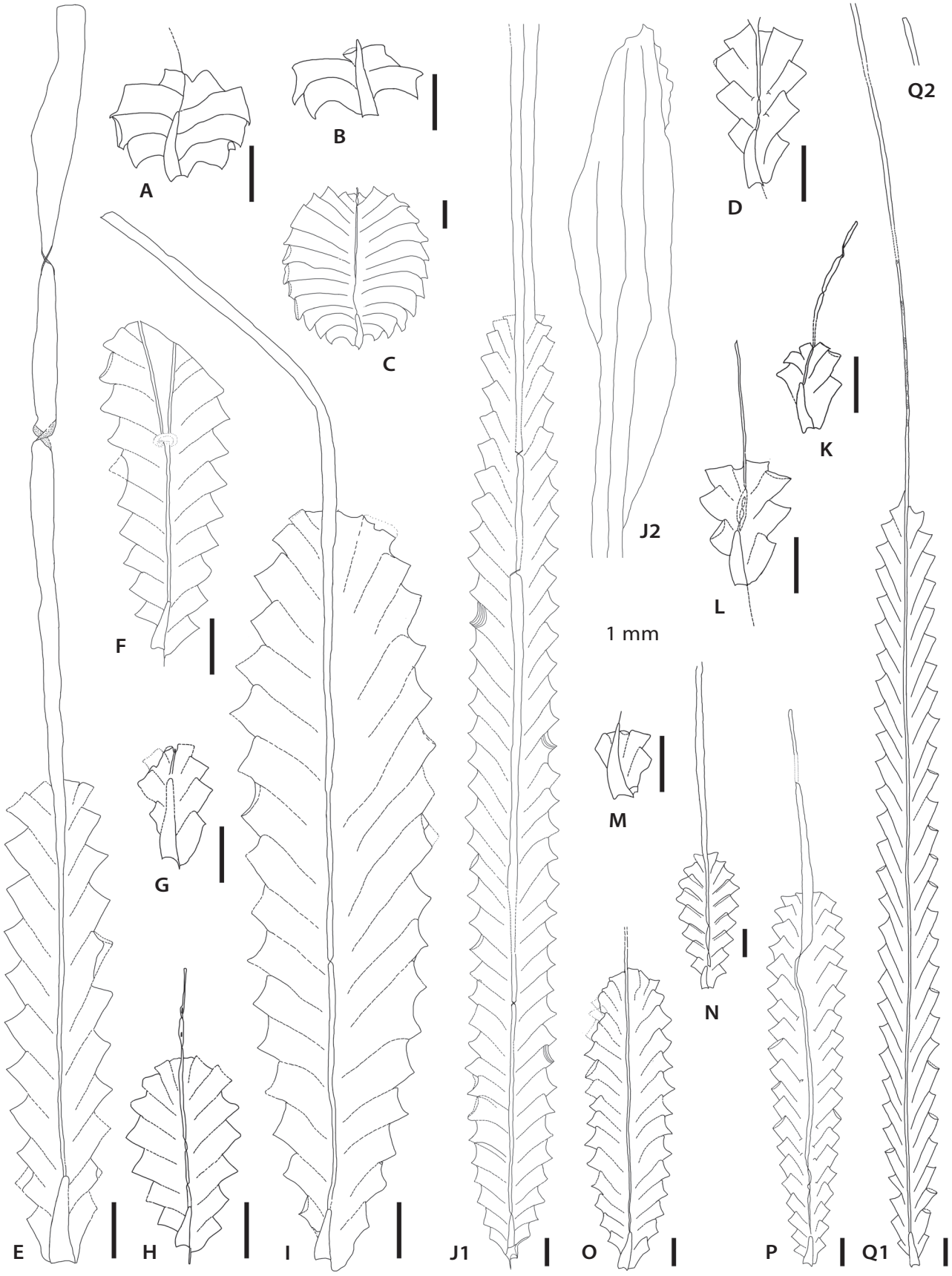
A
B
C
D
E
F
G
H
I
J1
J2
K
L
M
N
O
P
Q1
Q2
1 mm

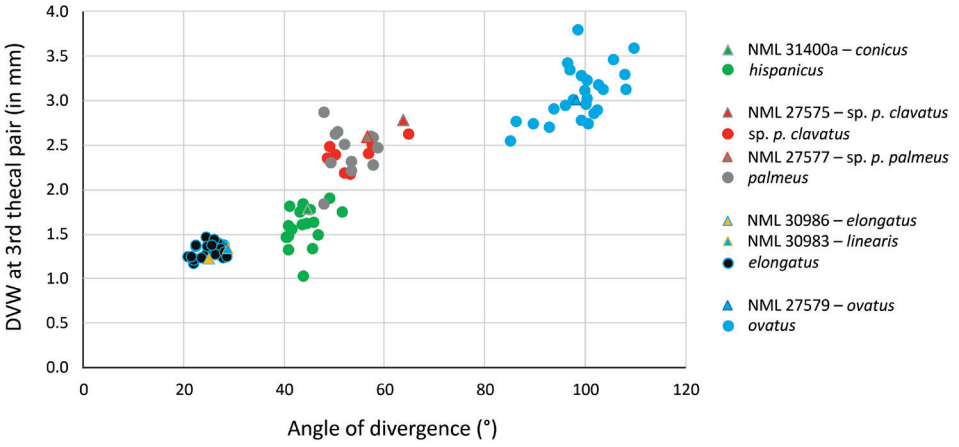

Figure 14. The angle of divergence of the 3rd thecal pair plotted against dorso-ventral width (DVW) in *P. hispanicus*, *P. palmeus*, *P. clavatus*, *P. elongatus*, *P. linearis* and *P. ovatus*. Type specimens are marked by triangles. Almost all specimens fall into one of four sets. Each individual set represents 1 species – *P. elongatus, P. hispanicus*, *P. palmeus* and *P. ovatus*. There are some aberrant specimens deviating from the average.

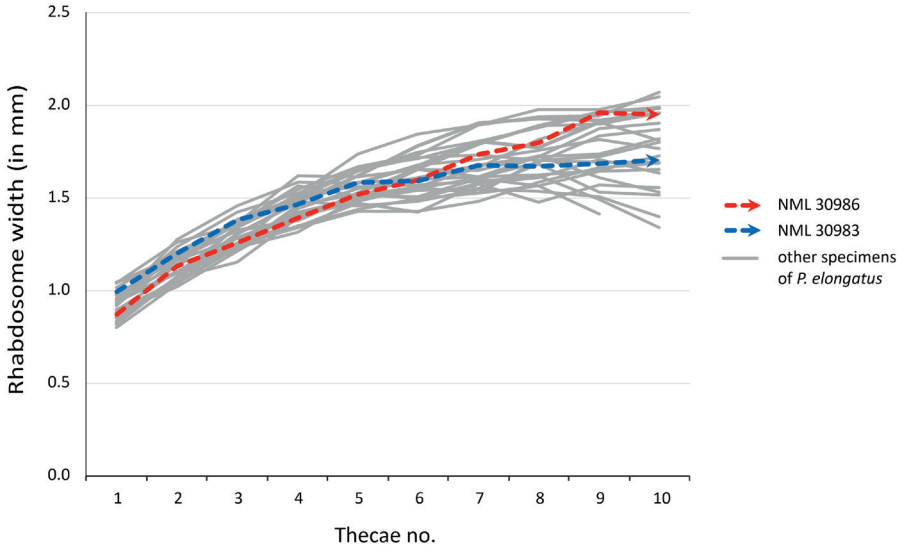

Figure 15. Graph showing rhabdosome width at specified thecae in type specimen of *P. elongatus linearis* (NML 30983), in type specimen of *P. elongatus elongatus* (NML 30986) and other specimens of *P. elongatus*. Both type specimens are housed at depositary of National Museum in Prague.

although they did not differ in any other parameter (*e.g.* angle of thecal apertures, angle of divergence). Various Ordovician forms of biserial graptolites, *e.g.* phyllograptids, possessing a markedly enlarged, oval proximal part, are well known (Maletz 2017, Maletz *et al.* 2018). This leads to the following questions. What causes this rhabdosome "widening" to occur in some specimens of a species? Is it a reaction to a sudden increase in nutrients in the living space? Or to the contrary, could the deformation of the rhabdosome be a result of parasitism, or, perhaps, a genetic defect? And how did it impact the movement of the colony in the water? The topics of parasitism, predation or movement in the water column have already been discussed by many authors, for example Kozłowski (1970), Underwood (1993) and Bates & Loydell (2000). The previously described abnormalities in rhabdosome growth were very clearly summarized by Muir (2011), and the overall distinction of parasitism in colonial organisms is addressed by Taylor (2015). However, the rhabdosome widening question is yet to be satisfactorily resolved.

Finally, the astogeny of *Parapetalolithus* should be discussed. In all species studied herein, specimens from a wide range of developmental stages were recorded, in

Figure 13. Selected adult and juvenile stages of all studied species of *Parapetalolithus* in this study: • A, B, C – *Parapetalolithus ovatus* (Barrande, 1850), ZAZ 45, ZAZ 44, ZAZ 51. • D, L, N, P – *Parapetalolithus hispanicus* (Haberfelner, 1931); ZAZ 19, ZAZ 16, ZAZ 71, ZAZ 73. • E, G – *Parapetalolithus tenuis* (Barrande, 1850); ZAZ 69, ZAZ 60. • F, H, I – *Parapetalolithus altissimus* (Elles & Wood, 1908); ZAZ 53, ZAZ 55, ZAZ 57. • J1–2, M, O – *Parapetalolithus palmeus* (Barrande, 1850); ZAZ 70, ZAZ 2, ZAZ 72. • K, Q1–2 – *Parapetalolithus elongatus* (Bouček & Přibyl, 1941a); ZAZ 28, ZAZ 33. • Specimens E–I originate from the *turriculatus* and *crispus* biozones from Litohlavy near Králův Dvůr. All other specimens originate from the *linnaei* Biozone of Želkovice, except for specimen J1–2 from the *linnaei* Biozone in Koněprusy. Scale bars represent 1 mm.

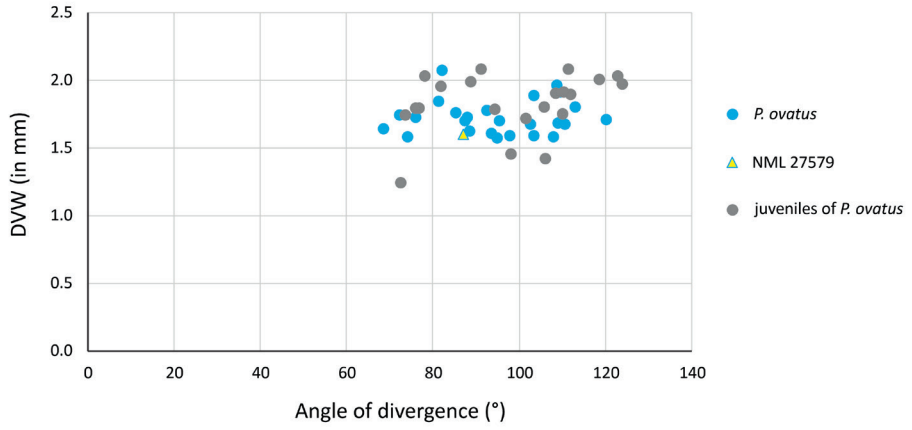

Figure 16. Angle of divergence (AD) and dorso-ventral width (DVW) comparison for the 1st pair of thecae of *P. ovatus*. Type specimen is marked by triangles. Adults of the species, the holotype of the species, and juveniles can be seen in one set. Species differentiation is possible already in the early stages of colony development.

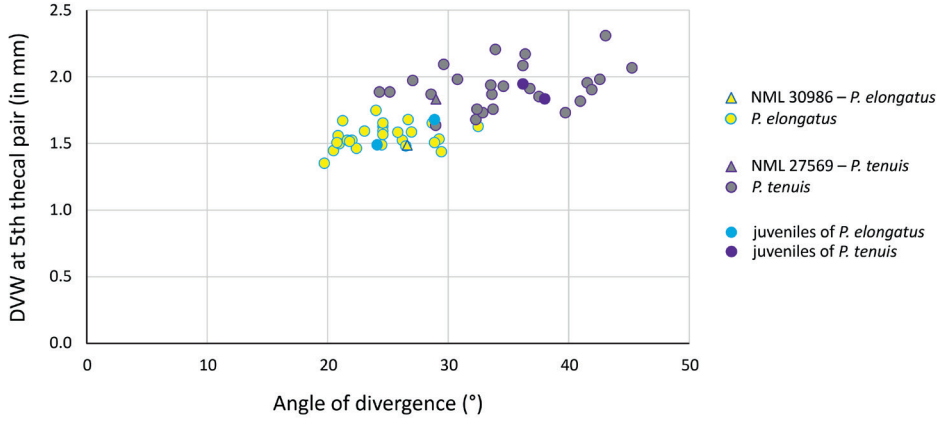

Figure 17. The angle of divergence of the 5th thecal pair plotted against dorso-ventral width in *P. elongatus* and *P. tenuis*. Type specimens are marked by triangles. Although these are two separate species from different biozones (*linnaei* and *turriculatus*), their sets partially overlap, and the holotypes of the species occur very close to each other. This indicates a possible close relationship between the two species.

which the growth of several pairs of thecae at the same time is clearly visible. However, specimens with visible growth of one pair of thecae only were also documented. A possible explanation is a reaction to the changing nutrient content in the environment: when nutrients were scarce in the environment, only one pair of thecae grew, and another pair of thecae began to grow only when it reached its final size. In contrast, when the amount of nutrients in the environment increased, the colony could "afford" to grow several pairs of thecae at the same time, *i.e.* before the previous pair of thecae reached the final size, another pair of thecae started to grow.

It is likely that the second option would be more advantageous for the movement of the colony in the water column as the rhabdosome would be lighter and more mobile.

Conclusions

(1) All species of the genus *Parapetalolithus*, from the *linnaei*, *turriculatus* and *crispus* biozones in the Prague Synform have been studied and revised. Of the original nine species and subspecies (*P. p. palmeus*, *P. p. clavatus*, *P. ovatus*, *P. e. elongatus*, *P. e. linearis*, *P. hispanicus*, *P. conicus*, *P. tenuis* and *P. altissimus*), only six species are recognised after the revision (*P. palmeus*, *P. ovatus*, *P. elongatus*, *P. hispanicus*, *P. tenuis* and *P. altissimus*).

(2) The representatives of a wide range of astogenetic stages were found in all species of *Parapetalolithus*. For the first time, detailed development series of astogenetic stages of the rhabdosome were compiled for all six studied species and for *Parapetalolithus* in general. Morphological intraspecific variability was also examined. These complete developmental series of individual *Parapetalolithus* species are unique not only because they capture the development of the colony in detail, but also because of their excellent preservation in the black shales.

(3) When preserved tectonically undeformed, *Parapetalolithus* species can be distinguished already in the very early juvenile stages of astogeny. The fossil record uncovers not only the individual stages in the development of the colony, but also the way it grew: several pairs of

thecae can grow at the same time, even though the older pairs of thecae have not yet reached their full size. It is possible that this was a reaction of the colony to a higher abundance of nutrients in the environment.

(4) When combined, angle of divergence (AD) and dorsoventral width (DVW) were the most suitable of the 12 measured parameters used for species identification. They also allow the determination of the degree of intraspecific variability of these characters in *Parapetalolithus*. Most noticeable were these interspecies differences and, conversely, the ranges of intraspecific variability when comparing AD and DVW values on the 3rd and 5th thecae across all species.

In contrast, the frequently utilized values $2TRD_2$ and $2TRD_5$ were neither well suited for distinguishing between individual species, although they are frequently used in the descriptions of different genera and species of graptolites.

(5) Morphological similarity and stratigraphical succession support a close evolutionary relationship between *Parapetalolithus elongatus* from the *linnaei* (*guerichi*) Biozone and *Parapetalolithus tenuis* from the *turriculatus* and *crispus* biozones (Fig. 17).

(6) Specimens with various forms of extended nema = nematularium (for instance, more or less spirally twisted ribbon-like structure) have been recorded in all six species studied; therefore, it cannot be a diagnostic feature distinguishing between the *Parapethalolithus* species.

Acknowledgements

The author was supported by a study scholarship at Charles University, to ensure financial support for travel associated with fieldwork. The research was also financed by Czech Science Foundation through project GA 20-23363S, and institutional support RVO 67985831 of the Institute of Geology of the Czech Academy of Sciences concerning the opportunity to use microscopic equipment and to study material deposited in the Czech Academy of Sciences. This manuscript contributes to the Strategic Research Plan of the Czech Geological Survey (DKRVO/ČGS 2023–2027) through internal project 311410. The author expresses gratitude for all the professional help provided by her supervisor, Petr Štorch. A big thank you also goes to my colleagues Martina Veselská Kočovská and Vojtěch Kovář for their unceasing support and lots of valuable advice. I also thank Štěpán Manda for his advice and observations with the figures. I also thank Martin Valent from the National Museum for his help in finding the type specimens. Many thanks also go to the two reviewers (David K. Loydell and S. Radzevičius) for their insightful comments and suggestions on the earlier version of the paper.

References

Barrande, J. 1850. *Graptolites de Bohême*. 74 pp. Privately published, Prague.

Bates, D.E.B. & Loydell, D.K. 2000. Parasitism on graptoloid graptolites. *Palaeontology 43(6)*, 1143–1151. DOI 10.1111/1475-4983.00164

Bjerreskov, M. 1975. Llandoverian and Wenlockian graptolites from Bornholm. *Fossils and Strata 8*, 1–94. DOI 10.18261/8200093921-1975-01

Bouček, B. 1932. Předběžná zpráva o některých nových druzích graptolitů z českého gotlandienu (část II). *Věstník Státního geologického ústavu 8(3)*, 150–155.

Bouček, B. 1933. Příspěvek k poznání graptolitů pásma komárovského (d) a šáreckého (d 1) českého ordoviku. *Věstník Státního geologického Ústavu Československé republiky 9*, 145–154.

Bouček, B. 1937. Graptolitová fauna českého spodního ludlowu. *Rozpravy České akademie věd a umění, Třída II 46(16)*, 1–26.

Bouček, B. & Münch, A. 1944. Die Retioliten des mitteleuropaischen Llandovery und unteren Wenlock. *Rozpravy České Akademie věd a umění, Třída II 53(41)*, 1–54.

Bouček, B. & Přibyl, A. 1941a. O rodu *Petalolithus* Suess z českého siluru. *Rozpravy České akademie věd a umění, Třída II 51(11)*, 1–22.

Bouček, B. & Přibyl, A. 1941b. O Petalolithech ze skupiny *P. folium* (His.) a o rodu *Cephalograptus* Hopk. *Rozpravy České Akademie věd a umění, Třída II 51(26)*, 1–22.

Bulman, O.M.B. 1955. *Graptolithina*, 101 pp. *In* Moore, R.C. (ed.) *Treatise on Invertebrate Paleontology, Part V*. Geological Society of America & University of Kansas Press, Lawrence.

Chen, X. 1984. Silurian graptolites from southern Shaanxi and northern Sichuan with special reference to classification of Monograptidae. *Palaeontologia Sinica*, *New Series B 166 (20)*, 1–102.

Chlupáč, I., Havlíček, V., Kříž, J., Kukal, Z. & Štorch, P. 1998. *Palaeozoic of the Barrandian (Cambrian to Devonian)*. 183 pp. Czech Geological Survey, Prague.

Elles, G.L. 1897. The subgenera *Petalograptus* and *Cephalograptus*. *Quarterly Journal of the Geological Society 53(1–4)*, 186–212. DOI 10.1144/GSL.JGS.1897.053.01-04.15

Elles, G.L., Wood, E.M. & Lapworth, C. 1908. A Monograph of British Graptolites. Part VII. *Monographs of the Palaeontographical Society 62(305)*, 121–358. DOI 10.1080/02693445.1908.12035543

Ge, M. 1990. Silurian graptolites from Chengkou, Sichuan. *Palaeontologica Sinica, New Series B 179(26)*, 1–157.

Gortani, M. 1923. Contribuzioni allo studio del Paleozoico Carnico. VII: Graptoliti del Monte Hochwipfel. *Palaeontographica Italica 29*, 1–24.

Gutiérrez-Marco, J.C. & Štorch, P. 1998. Graptolite biostratigraphy of the lower Silurian (Llandovery) shelf deposits

of the Western Iberian Cordillera, Spain. *Geological Magazine 135(1)*, 71–92. DOI 10.1017/S0016756897007802

Haberfelner, E. 1931. Eine revision der Graptolithen der Sierra Morena (Spanien). *Abhandlungen der Senckenbergischen Naturforschenden Gesellschaft 43*, 19–66.

Havlíček, V. 1981. Development of a linear sedimentary depression exemplified by the Prague Basin (Ordovician-Middle Devonian; Barrandian area-central Bohemia). *Sborník geologických věd, Geologie 35*, 7–48.

Havlíček, V. 1982. Ordovician in Bohemia: development of the Prague Basin and its benthic communities. *Sborník geologických věd, Řada geologie 37*, 103–136.

Hopfensperger, B., Maletz, J., Lukeneder, P., Heinz, P. & Ottner, F. 2021. Early graptolite research: Eduard Suess and the Bilimek collection. *Bulletin of Geosciences 96(3)*, 279–293. DOI 10.3140/bull.geosci.1829

Howe, M.P.A. 1983. Measurement of thecal spacing in graptolites. *Geological Magazine 120*, 635–638. DOI 10.1017/S0016756800027795

Hundt, R. 1924. *Die Graptolithen des deutschen Silurs*. 96 pp. Verlag Max Weg, Leipzig.

Hundt, R. 1957. Schwebeblasen bei Graptolithen (Diplograptidae) ein Beitrag zu ihrer Lebensweise. *200 Jahre Naturkundesmuseum. Heidecksburg*, 79–95.

Hutt, J.E. 1974. The Llandovery graptolites of the English Lake District. Part 1. *Monographs of the Palaeontographical Society 128(540)*, 1–60. DOI 10.1080/25761900.2022.12131726

Koren', T.N. & Rickards, R.B. 1996. Taxonomy and evolution of Llandovery biserial graptoloids from the southern Urals, western Kazakhstan. *Special Papers in Palaeontology 54*, 1–103.

Kozłowski, R. 1970. Tubotheca – a peculiar morphological element in some graptolites. *Acta palaeontologica polonica 15(4)*, 393–410.

Kříž, J. 1975. Revision of the Lower Silurian stratigraphy in Central Bohemia. *Věstník Ústředního ústavu geologického 50*, 275–282.

Kříž, J. 1992. Silurian field excursions: Prague Basin (Barrandian), Bohemia. *National Museum of Wales, Geological Series 13*, 1–111.

Lapworth, C. 1873. Notes on the British graptolites and their allies. 1. On an improved classification of the Rhabdophora, part 2. *Geological Magazine 10*, 555–560. DOI 10.1017/S0016756800469372

Lenz, A.C. & Kozłowska-Dawidziuk, A. 2004. *Ludlow and Pridoli (Upper Silurian) graptolites from the Arctic Islands, Canada*. 141 pp. NRC Research Press, Ottawa, Canada. DOI 10.1139/9780660193267

Lenz, A.C., Bates, D.E.B., Kozłowska, A. & Maletz, J. 2018. Part V, second revision, Chapter 26: Family Retiolitidae: Introduction, morphology, and systematic descriptions. *Treatise Online 114*, 1–37. DOI 10.17161/to.v0i0.8249

Loydell, D.K. 1992. Upper Aeronian and lower Telychian (Llandovery) graptolites from western Mid-Wales. I. *Monograph of the Palaeontographical Society 146(589)*, 1–55. DOI 10.1080/25761900.2022.12131772

Loydell, D.K., Männik, P. & Nestor, V. 2003. Integrated biostratigraphy of the lower Silurian of the Aizpute-41 core, Latvia. *Geological Magazine 140(2)*, 205–229. DOI 10.1017/S0016756802007264

Loydell, D.K., Nestor, V. & Männik, P. 2010. Integrated biostratigraphy of the lower Silurian of the Kolka-54 core, Latvia. *Geological Magazine 147(2)*, 253–280. DOI 10.1017/S0016756809990574

Loydell, D.K., Frýda, J. & Gutiérrez-Marco, J.C. 2015. The Aeronian/Telychian (Llandovery, Silurian) boundary, with particular reference to sections around the El Pintado reservoir, Seville Province, Spain. *Bulletin of Geosciences 90(4)*, 743–794. DOI 10.3140/bull.geosci.1564

Loydell, D.K., Walasek, N., Schovsbo, N.H. & Nielsen, A.T. 2017. Graptolite biostratigraphy of the lower Silurian of the Sommerodde-1 core, Bornholm, Denmark. *Bulletin of the Geological Society of Denmark 65*, 135–160. DOI 10.37570/bgsd-2017-65-09

Maletz, J. 2017. *Graptolite paleobiology.* 323 pp. Wiley Blackwell, Oxford. DOI 10.1002/9781118515624

Maletz, J., Toro, B.A., Zhang, Y. & Vandenberg, A.H. 2018. Part V, Second Revision, Chapter 20: Suborder Dichograptina: Introduction, morphology, and systematic descriptions. *Treatise Online 108*, 1–28. DOI 10.17161/to.v0i0.7736

Maletz, J., Wang, C., Kai, W. & Wang, X. 2021. Upper Ordovician (Hirnantian) to lower Silurian (Telychian, Llandovery) graptolite biostratigraphy of the Tielugou section, Shennongjia anticline, Hubei Province, China. *PalZ 95(3)*, 453–481. DOI 10.1007/s12542-020-00544-5

Melchin, M.J. 1998. Morphology and phylogeny of some early Silurian 'diplograptid' genera from Cornwallis Island, Arctic Canada. *Palaeontology 41(2)*, 263–315.

Melichar, R. 2004. Tectonics of the Prague Synform: a hundred years of scientific discussion. *Krystalinikum 30*, 167–187.

Muir, L.A. 2011. An unusual specimen of *Glyptograptus* from Dob's Linn (Southern Uplands, Scotland), and a discussion of graptolite teratomorphies. *Proceedings of the Yorkshire Geological Society 58(4)*, 311–317. DOI 10.1144/pygs.58.4.294

Paškevičius, J. 1979. *Biostratigrafija i graptolity silura Litvy:* 268 pp. Mokslas, Vilnius. [in Russian]

Perner, J. 1897. Study of the graptolites of Bohemia. *Palaeontographica Bohemiae 1897*, 1–54.

Přibyl, A. 1948. Bibliographic index of Bohemian Silurian graptolites. *Knihovna Státního Geologického Ústavu České Republiky 22*, 1–96.

Röhlich, P. 2007. Structure of the Prague Basin: The deformation diversity and its causes (the Czech Republic). *Bulletin of Geosciences 82(2)*, 175–182. DOI 10.3140/bull.geosci.2007.02.175

Schauer, M. 1971. Biostratigraphie und Taxionomie der Graptolithen des tieferen Silurs unter besonderer Berücksichtigung der tektonischen Deformation. *Freiberger Forschungshefte Reihe C 373*, 1–185.

Štorch, P. 1992. Some new and little known graptolites from the Lower Silurian of Bohemia (Prague Basin, Barrandian Area). *Časopis pro mineralogii a geologii 37(3)*, 193–201.

Štorch, P. 1998. New data on Telychian (Upper Llandovery, Silurian) graptolites from Spain. *Journal of the Czech Geological Society 43(3)*, 113–142.

Štorch, P. 2006. Facies development, depositional settings and sequence stratigraphy across the Ordovician-Silurian boundary: a new perspective from Barrandian area of the Czech Republic. *Geological Journal 41*, 163–192. DOI 10.1002/gj.1038

Štorch, P. 2023. Graptolite biostratigraphy and biodiversity dynamics in the Silurian System of the Prague Synform (Barrandian area, Czech Republic). *Bulletin of Geosciences 98(1)*, 1–78. DOI 10.3140/bull.geosci.1862

Štorch, P. & Kraft, P. 2009. Graptolite assemblages and stratigraphy of the lower Silurian Mrákotín Formation, Hlinsko Zone, NE interior of the Bohemian Massif (Czech Republic). *Bulletin of Geosciences 84(1)*, 51–74. DOI 10.3140/bull.geosci.1077

Štorch, P. & Massa, D. 2003. Biostratigraphy, correlation, environmental and biogeographic interpretation of the Lower Silurian graptolite faunas of Libya. *The geology of northwest Libya 1*, 237–251.

Štorch, P. & Piras, S. 2009. Silurian graptolites of Sardinia: assemblages and biostratigraphy, 77–93. *In* Corradini, C., Ferretti, A. & Štorch, P. (eds) *Silurian of Sardinia*. *Rendiconti della Societa Paleontologica Italiana 3(1).*

Štorch, P., Loydell, D.K., Melchin, M.J. & Goldman, D. in print. Graptolites in biostratigraphy: the primary tool for subdivision and correlation of Ordovician, Silurian, and Lower Devonian offshore marine successions. *Newsletters on Stratigraphy.*

Štorch, P., Manda, Š., Tasáryová, Z., Frýda, J., Chadimová, L. & Melchin, M. J. 2018. A proposed new global stratotype for Aeronian Stage of the Silurian System: Hlásná Třebaň section, Czech Republic. *Lethaia 51(3)*, 357–388. DOI 10.1111/let.12250

Suess, E. 1851. Über böhmische Graptolithen. *Naturwissenschaftlichen Abhandlungen herausgegeben vom W. Haidinger*, *Wien*, 1–50.

Suyarkova, A.A. 2017. Biostratigrafiya nizhnesilurijskikh otlozhenii Kaliningradskoy oblasti po graptolitam. *Trudy VSEGEI, New series 358*, 1–126. [in Russian]

Taylor, P.D. 2015. Differentiating parasitism and other interactions in fossilized colonial organisms. *Advances in Parasitology 90*, 329–347. DOI 10.1016/bs.apar.2015.05.002

Underwood, C.J. 1993. The position of graptolites within Lower Palaeozoic planktic ecosystems. *Lethaia 26(3)*, 189–202. DOI 10.1111/j.1502-3931.1993.tb01517.x

Vacek, F. & Žák, J. 2017. A lifetime of the Variscan orogenic plateau from uplift to collapse as recorded by the Prague Basin, Bohemian Massif. *Geological Magazine 156(3)*, 1–25. DOI 10.1017/S0016756817000875

Williams, M., Zalasiewicz, J., Boukhamsin, H. & Cesari, C. 2016. Early Silurian (Llandovery) graptolite assemblages of Saudi Arabia: biozonation, palaeoenvironmental significance and biogeography. *Geological Quarterly 60(1)*, 3–25. DOI 10.7306/gq.1270

Zalasiewicz, J.A. & Rushton, A.W.A. (eds) 2008. *Atlas of Graptolite Type Specimens, Folio 2.* 100 pp. The Palaeontographical Society and the British and Irish Graptolite Group, Maidenhead.

Zalasiewicz, J.A., Rushton, A.W.A., Hutt, J.E. & Howe, M.P.A. 2000. *Atlas of Graptolite Type Specimens, Folio 1.* 100 pp. Michael Heath Limited, Reigate, Surrey.